Mathematical Biosciences 278 (2016) 63–76

Contents lists available at ScienceDirect

Mathematical Biosciences

journal homepage: www.elsevier.com/locate/mbs

A piecewise model of virus-immune system with two thresholds

Biao Tang[a,b], Yanni Xiao[a,*], Jianhong Wu[b]

[a] School of Mathematics and Statistics, Xi'an Jiaotong University, Xi'an 710049, PR China
[b] Centre for Disease Modelling, York Institute for Health Research, York University, Toronto, ON M3J 1P3, Canada

ARTICLE INFO

Article history:
Received 10 July 2015
Revised 10 March 2016
Accepted 10 June 2016
Available online 16 June 2016

Keywords:
Structured treatment interruptions
Two thresholds
Piecewise model
Global dynamics
HIV

ABSTRACT

The combined antiretroviral therapy with interleukin (IL)-2 treatment may not be enough to preclude exceptionally high growth of HIV virus nor rebuilt the HIV-specific CD4 or CD8 T-cell proliferative immune response for management of HIV infected patients. Whether extra inclusion of immune therapy can induce the HIV-specific immune response and control HIV replication remains challenging. Here a piecewise virus-immune model with two thresholds is proposed to represent the HIV-1 RNA and effector cell-guided therapy strategies. We first analyze the dynamics of the virus-immune system with effector cell-guided immune therapy only and prove that there exists a critical level of the intensity of immune therapy determining whether the HIV-1 RAN virus loads can be controlled below a relative low level. Our analysis of the global dynamics of the proposed model shows that the pseudo-equilibrium can be globally stable or locally bistable with order 1 periodic solution or bistable with the virus-free periodic solution under various appropriate conditions. This indicates that HIV viral loads can either be eradicated or stabilize at a previously given level or go to infinity (corresponding to the effector cells oscillating), depending on the threshold levels and the initial HIV virus loads and effector cell counts. Comparing with the single threshold therapy strategy we obtain that with two thresholds therapy strategies either virus can be eradicated or the controllable region, where HIV viral loads can be maintained below a certain value, can be enlarged.

1. Introduction

Lifelong highly active antiretroviral therapy (HAART) continues to be associated with many problems such as adherence difficulties and evolution of drug resistance [1–4]. Structured therapy interruptions (STIs) have been suggested as being capable of achieving sustained specific immunity for early therapy in HIV infection. As an alternative strategy, STI is a good choice for some chronically infected individuals who may need to take drugs throughout their lives, and it is beneficial for the patients' immune reconstruction during the period when they are not taking the drugs [5].

Recently, to compare STI strategies with the continuous antiretroviral therapy, several clinical studies have been done with conflicting results [5–12]. In particular, Ruiz et al. [12] designed an experiment to evaluate the safety of CD4 cell counts and plasma HIV-1 RNA-guided structured treatment interruptions (STIs) aiming to maintain CD4 T cell counts higher than 350 cells/μl and plasma HIV-1 RNA less than 100,000 copies/μl. Although many mathematical models have been formulated to model continuous therapy [13–15], few attempts have been made to model structured treatment interruptions. In 2012, Tang et al. [16] proposed a piecewise system to describe the CD4 cell-guided STIs, to quantitatively explore STI strategies and to investigate the virus dynamics under these strategies. This system has offered explanations for some controversial conclusions from different clinical studies. In 2015, by considering combined antiretroviral therapy with interleukin (IL)-2 treatment, we proposed a piecewise virus-immune dynamic model with HIV-1 RNA-guided therapy [17]. This model is given as follows:

$$\begin{cases} \left.\begin{aligned} x' &= rx - pxy, \\ y' &= \frac{cxy}{1+\omega x} - qxy - \delta y, \end{aligned}\right\} x < V_s, \\ \left.\begin{aligned} x' &= rx - pxy - \epsilon_1 x, \\ y' &= \frac{cxy}{1+\omega x} - qxy - \delta y + \epsilon_2 y, \end{aligned}\right\} x > V_s, \end{cases} \tag{1}$$

where x and y represent the HIV virus loads and the density of effector cells, respectively. V_s is the critical value of HIV virus loads determining whether the therapy is carried out or not. Here ϵ_1 represents the rate of elimination of HIV virus due to antiretroviral therapy and ϵ_2 denotes the growth rate of the effector cells due to interleukin (IL)-2 treatment. r denotes the growth rate of HIV virus which incorporates both multiplication and death of HIV

* Corresponding author. Tel.: +86 2982663938; fax: +86 2982663938.
E-mail address: yxiao@mail.xjtu.edu.cn, yannixiao317@hotmail.com (Y. Xiao).

http://dx.doi.org/10.1016/j.mbs.2016.06.003
0025-5564/

virus, δ is the death rate of the effector cells, p denotes the rate of binding of the effector cells to the HIV viruses. When interacting with the HIV virus, the effector cells usually have a limited ability to repeatedly kill the virus because the virus can also inhibit the activity of immune cells. Here q represents the rate of inactivation of the effector cells. $cx/(1+\omega x)$ denotes the rate at which effector cells accumulate due to the immune response.

In the paper [17], we concluded that proper combinations of threshold and initial HIV virus loads and effector cell counts can successfully preclude exceptionally high growth of HIV virus and, in particular, maximize the controllable region. However, whatever the threshold is, depending on the initial conditions of patients' HIV virus can not be eradicated but even increase to infinity, which means that the combined antiretroviral therapy with interleukin (IL)-2 treatment may not be enough to rebuild the HIV-specific CD4 or CD8 T-cell proliferative immune response for management of HIV infected patients. In [18], the authors developed a clinic experiment studying combined antiretroviral therapy and interleukin (IL)-2 treatment with immune therapy. The patients were divided into four groups, in which the group C simultaneously received antiretroviral therapy, interleukin (IL)-2 treatment and immune therapy with HIV vaccine was injected once every 3 months. They showed that interleukin (IL)-2 treatment and immune therapy can induce the HIV-specific immune response. How the impulsive immune therapy affects the dynamics of virus-immune system with HIV-1 RNA-guided therapy and whether the inclusion of impulsive immune therapy can maintain the virus below a certain level, remain unclear. Addressing these issues through a mathematical modeling framework falls within the scope of this study.

More precisely, the purpose of this study is to propose a mathematical model to describe the combined antiretroviral therapy and interleukin (IL)-2 treatment with immune therapy. We address such challenging questions as whether the comprehensive therapy under the HIV-1 RNA and effector cell-guided structured treatment can successfully inhibit replication of HIV virus and rebuild the HIV-specific CD4 or CD8 T-cell proliferative immune response, and whether the therapy can control HIV-1 RNA below a certain level and maintain the density of effector cells above a certain level. The rest parts of this paper is organized as follows. In Section 2, we formulate a piecewise virus-immune model with two thresholds and introduce the relative definitions. The dynamics of the proposed model with either only the effector cell or the HIV-1 RNA-guided therapy is discussed in Section 3. Then, in Section 4, we investigate the global dynamics of the proposed model. Finally, we conclude the paper with some remarks.

2. Model formulation and preliminaries

In this paper, we formulate the model that incorporate both the antiretroviral therapy and interleukin (IL)-2 treatment under the assumption that whenever the virus load exceeds the critical level (i.e. V_s), antiretroviral drugs are applied to inhibit the growth of the virus, and simultaneously interleukin (IL)-2 treatment is used [17]. The immune therapy mainly aims at rebuilding the HIV-special T cell immune response and guaranteeing the density of effector cells is enough to control the growth of HIV virus. Thus, there can be a critical value of the density of effector cells, denoted by T_s, determining whether the immune therapy is carried out. In particular, the immune therapy isn't carried out when the density of the effector cells is above the level T_s and one dose of HIV vaccine is injected immediately once the density of the effector cells declines to the level T_s. Let ρ represent the intensity of the immune therapy every time with $\rho \geq 1$. Therefore, based on model (1), we have proposed the following formulation:

$$\begin{cases} \left.\begin{cases} x' = rx - pxy, \\ y' = \frac{cxy}{1+\omega x} - qxy - \delta y, \end{cases}\right\} y > T_s, \\ \left.\begin{cases} x(t^+) = x(t), \\ y(t^+) = \rho y(t), \end{cases}\right\} y = T_s, \end{cases} \Bigg\} x < V_s, \quad \begin{cases} \left.\begin{cases} x' = rx - pxy - \epsilon_1 x, \\ y' = \frac{cxy}{1+\omega x} - qxy - \delta y + \epsilon_2 y, \end{cases}\right\} y > T_s, \\ \left.\begin{cases} x(t^+) = x(t), \\ y(t^+) = \rho y(t), \end{cases}\right\} y = T_s, \end{cases} \Bigg\} x > V_s. \tag{2}$$

Before going further discussing the dynamics of system (2), we now introduce some technical definitions.

Let $R^2_+ = \{X = (x, y) | x \geq 0, y \geq 0\}$. A generic planar Filippov system is defined as follows [19–26]:

$$\dot{X} = \begin{cases} F_{D_1}(X), & X \in D_1, \\ F_{D_2}(X), & X \in D_2, \end{cases} \tag{3}$$

where $D_1 = \{X \in R^2_+ | H(X) < 0\}$ and $D_2 = \{X \in R^2_+ |\ H(X) > 0\}$ with $H(X)$ as a smooth scale function.

Definition 1. A point X^* is called a regular equilibrium of system (3) if $F_{D_1}(X^*) = 0,\ H(X^*) < 0$ or $F_{D_2}(X^*) = 0,\ H(X^*) > 0$ while it is called a virtual equilibrium of system (3) if $F_{D_1}(X^*) = 0,\ H(X^*) > 0$ or $F_{D_2}(X^*) = 0,\ H(X^*) < 0$.

Definition 2. A point X^* is called a pseudo-equilibrium if it is an equilibrium of the sliding mode of system (3), i.e. $\lambda F_{D_1}(X^*) + (1-\lambda)F_{D_2}(X^*) = 0, H(X^*) = 0$ with $0 < \lambda < 1$ and

$$\lambda = \frac{\langle H_X(X^*), F_{D_2}(X^*)\rangle}{\langle H_X(X^*), F_{D_2}(X^*) - F_{D_1}(X^*)\rangle}.$$

A generalized planar impulsive semi-dynamic system can be defined as follows [27–33]:

$$\begin{cases} \frac{dx}{dt} = P(x, y),\ \frac{dy}{dt} = Q(x, y), if\ \phi(x, y) \neq 0, \\ \triangle x = a(x, y),\ \triangle y = b(x, y), if\ \phi(x, y) = 0, \end{cases} \tag{4}$$

where $(x, y) \in R^2_+$, $\triangle x = x^+ - x$ and $\triangle y = y^+ - y$. P, Q, a, b are continuous functions from R^2_+ into R_+. The impulsive function $I : R^2_+ \to R^2_+$ is defined as follows:

$$I(x, y) = (I_1(x, y), I_2(x, y)) = (x + a(x, y), y + b(x, y)),$$

and $Z^+ = (x^+, y^+)$ is called an impulsive point of $Z = (x, y)$.

Let (R^2_+, π) be a planar semi-dynamic system. For any $Z \in R^2_+$, the positive orbit of Z is given by $C^+(z) = \{\pi(Z, t) | t \in R_+\}$ which is denoted by $\pi^+(Z)$. And we define $F(Z, t) = \{Z' | \pi(Z', t) = Z\}$ for $t \geq 0$ and $Z \in R^2_+$.

Definition 3. A planar impulsive semi-dynamic system $(R^2_+, \pi; M, I)$ consists of a continuous semi-dynamic system (R^2_+, π) together with a nonempty closed subset M of R^2_+ and a continuous function $I : M \to R^2_+$ such that for every $Z \in M$, there exists a $\epsilon_Z > 0$ such that

$$F(Z, (0, \epsilon_Z)) \cap M = \emptyset \quad \text{and} \quad \pi(Z, (0, \epsilon_Z)) \cap M = \emptyset.$$

Definition 4. A trajectory $\pi^+(Z)$ of $(R^2_+, \pi; M, I)$ is said to be order k periodic if there exist nonnegative integers m and k such that k is the smallest integer for which $I^m(Z) = I^{m+k}(Z)$ with $Z \in M$.

Definition 5. The Lambert W function [34] is defined to be a multivalued inverse of the function $z \mapsto ze^z$ satisfying

$$\text{LambertW}(z)\exp(\text{LambertW}(z)) = z.$$

And we denote it as W for simplicity. Note that the function $z\exp(z)$ has the positive derivative $(z+1)\exp(z)$ when $z > -1$. Define the inverse function of $z\exp(z)$ restricted on the interval

$[-1,+\infty)$ to be $W(0,z)$. Similarly, we define the inverse function of $z\exp(z)$ restricted on the interval $(-\infty,-1]$ to be $W(-1,z)$. The branch $W(0,z)$ is defined on the interval $[-e^{-1},+\infty)$ and it is monotonically increasing with respect to z. And the branch $W(-1,z)$ is defined on the interval $[-e^{-1},0)$ and it is a monotonically decreasing function with respect to z.

3. Dynamics of system (2) with only one of the threshold strategies is considered

3.1. Properties of system (2) with only the effector cell-guided therapy considered

When only the effector cell-guided therapy is considered, there are two different choices for therapy: one is that we do not carry out the antiretroviral therapy and interleukin (IL)-2 treatment; the other is that the antiretroviral therapy and interleukin (IL)-2 treatment are always carried out. From the mathematical point of view, these strategies correspond to the cases of a critical value V_s satisfying $V_s=0$ or $V_s=+\infty$. Then system (2) becomes two generalized planar impulsive semi-dynamic systems as follows

$$\begin{cases} \left.\begin{aligned} x' &= rx-pxy,\\ y' &= \frac{cxy}{1+\omega x}-qxy-\delta y, \end{aligned}\right\} y>T_s,\\ \left.\begin{aligned} x(t^+) &= x(t),\\ y(t^+) &= \rho y(t), \end{aligned}\right\} y=T_s, \end{cases} \tag{5}$$

and

$$\begin{cases} \left.\begin{aligned} x' &= rx-pxy-\epsilon_1 x,\\ y' &= \frac{cxy}{1+\omega x}-qxy-\delta y+\epsilon_2 y, \end{aligned}\right\} y>T_s,\\ \left.\begin{aligned} x(t^+) &= x(t),\\ y(t^+) &= \rho y(t), \end{aligned}\right\} y=T_s. \end{cases} \tag{6}$$

We first consider the dynamical behaviors of these systems without any impulse. In the absence of impulse systems (5) and (6) give

$$(S_1)\qquad \begin{cases} x' = rx-pxy,\\ y' = \frac{cxy}{1+\omega x}-qxy-\delta y, \end{cases} \tag{7}$$

and

$$(S_2)\qquad \begin{cases} x' = rx-pxy-\epsilon_1 x,\\ y' = \frac{cxy}{1+\omega x}-qxy-\delta y+\epsilon_2 y. \end{cases} \tag{8}$$

For convenience, we denote model (7) as system S_1 and model (8) as system S_2. Through simple calculations, we have that if $c-q-\delta\omega>2\sqrt{q\delta\omega}$, $\delta>\epsilon_2$ and $r>\epsilon_1$ hold true, then system $S_1(S_2)$ exists two positive equilibria, denoted by $E^1_{S_1}=(x^1_{S_1},y^1_{S_1})$ and $E^2_{S_1}=(x^2_{S_1},y^2_{S_1})$ ($E^1_{S_2}=(x^1_{S_2},y^1_{S_2})$ and $E^2_{S_2}=(x^2_{S_2},y^2_{S_2})$), respectively. Here we have

$$x^i_{S_1}=\frac{c-q-\delta\omega\mp\sqrt{(c-q-\delta\omega)^2-4q\delta\omega}}{2q\omega},\ y^i_{S_1}=\frac{r}{p},\ i=1,2 \tag{9}$$

and

$$x^i_{S_2}=\frac{c-q-(\delta-\epsilon_2)\omega\mp\sqrt{(c-q-(\delta-\epsilon_2)\omega)^2-4q(\delta-\epsilon_2)\omega}}{2q\omega},\quad y^i_{S_2}=\frac{r-\epsilon_1}{p} \tag{10}$$

with $x^1_{S_2}<x^1_{S_1}<x^2_{S_1}<x^2_{S_2}$. It is easy to prove that the equilibrium $E^1_{S_1}$ is a center and $E^2_{S_1}$ is a saddle point for the linear system of system S_1 by checking the corresponding eigenvalues. Further, we find that the system S_1 has a first integral, which is shown in the proof of Lemma 1 in details. Therefore, we have that the equilibrium $E^1_{S_1}$ is a center of system S_1 and $E^2_{S_1}$ is a saddle point of system S_1. The similar properties hold for system S_2. Thus, the existence and stability of the equilibria of the two systems when $c-q-\delta\omega>2\sqrt{q\delta\omega}$, $\delta>\epsilon_2$ and $r>\epsilon_1$ are stated as follows.

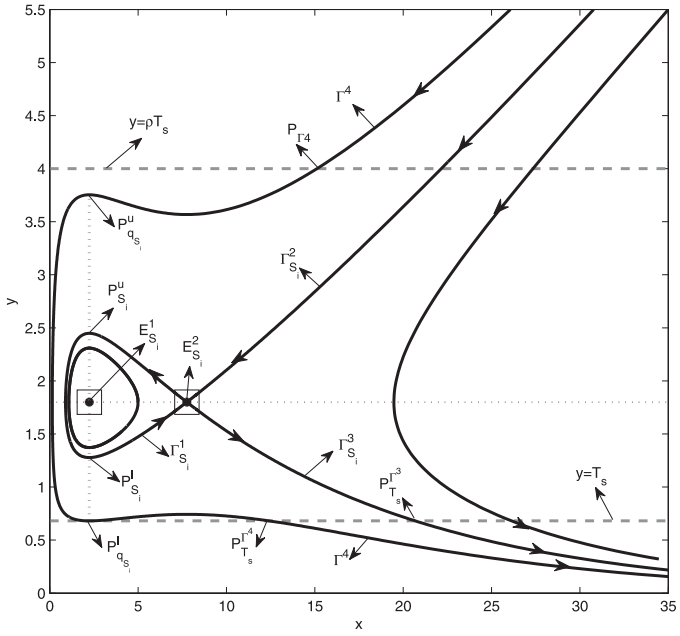

Fig. 1. The dynamical behaviors of systems S_1 and S_2 while there are two positive equilibria.

Proposition 1. *For system S_1 (S_2) there exists a trivial equilibrium $E^0_{S_1}=(0,0)$ ($E^0_{S_2}=(0,0)$) which is a saddle point; If $c-q-\delta\omega>2\sqrt{q\delta\omega}$, $\delta>\epsilon_2$ and $r>\epsilon_1$ hold true, system S_1 (S_2) has two positive equilibria $E^1_{S_1}$ ($E^1_{S_2}$) which is a center, and $E^2_{S_1}$ ($E^2_{S_2}$) which is a saddle point. Also, there exists a homoclinic orbit with respect to $E^2_{S_1}$ ($E^2_{S_2}$), denoted as $\Gamma^1_{S_1}$ ($\Gamma^1_{S_2}$). The other one dimension stable and unstable manifold of the saddle point $E^2_{S_i}$ is denoted by $\Gamma^2_{S_i}$ and $\Gamma^3_{S_i}$, respectively. The topological structure of the orbits of both systems is shown in Fig. 1.*

In the rest of this paper, we assume that $c-q-\delta\omega>2\sqrt{q\delta\omega}$, $\delta>\epsilon_2$ and $r>\epsilon_1$ always hold true. According to the topological structure of system S_1 (S_2), there must be an orbit, denoted by Γ^4, which is tangent to the line $y=T_s$ at the point $P^l_{q_{S_1}}(x^1_{S_1},T_s)$ ($P^l_{q_{S_2}}(x^1_{S_2},T_s)$) as shown in Fig. 1. Let the other intersection point between the orbit Γ^4 and the line $x=x^1_{S_1}$ ($x=x^1_{S_2}$) be $P^u_{q_{S_1}}(x^1_{S_1},y^u_{q_{S_1}})$ ($P^u_{q_{S_2}}(x^1_{S_2},y^u_{q_{S_2}})$). From Proposition 1, we can see that when $\rho-q-\delta\omega>2\sqrt{q\delta\omega}$, $\delta>\epsilon_2$ and $r>\epsilon_1$ hold true, systems S_1 and S_2 are topologically equivalent. Therefore, without loss of generality, we mainly discuss the dynamics of system S_1 with impulse, that is system (5). Denote the region bounded by the orbits $\Gamma^1_{S_i}$ as $D_{\Gamma^1_{S_i}}$ and the intersection points of the low branch and the upper branch of the orbit $\Gamma^1_{S_i}$(i=1,2) to the line $x=x^1_{S_i}$ as $P^l_{S_i}=(x^1_{S_i},y^l_{S_i})$ and $P^u_{S_i}=(x^1_{S_i},y^u_{S_i})$, respectively. As we can see from Fig. 1, $E^1_{S_i}$ is stable in the region $D_{\Gamma^1_{S_i}}$, which means that within the region $D_{\Gamma^1_{S_i}}$ both the virus loads and the effector cell counts can maintain in a certain range without any immune therapy. Therefore, it is reasonable to assume that $T_s<\min\{y^l_{S_1},y^l_{S_2}\}$.

Theorem 1. *In system (5), there exists a virus-free periodic solution.*

Proof. Let $x = 0$, then system (5) becomes the following

$$\begin{cases} y' = -\delta y, y > T_s, \\ y(t^+) = \rho y(t), y = T_s. \end{cases} \tag{11}$$

Integrating the first equation of (11) with the initial condition $y(0^+) = \rho T_s$, yields

$$y(t) = \rho T_s e^{-\delta t}.$$

Let $\rho T_s e^{-\delta T} = T_s$ and solving it with respect to T we get the period T_0 with $T_0 = \frac{1}{\delta}\ln(\rho)$. Therefore, the model (11) has an order-1 periodic solution, denoted as $\xi(t)$ and $\xi(t) = \rho T_s e^{-\delta t}$ with period T_0, which means that system (5) possesses a virus-free periodic solution $\zeta_{S_1}(t) = (0, \xi(t))$. The proof is completed. □

Lemma 1. *Set Γ_L and Γ_N be two orbits of system S_1 which intersect with the line $y = T_s$ at $L_1(x_{L_1}, T_s)$ and $N_1(x_{N_1}, T_s)$ respectively. Let $L_2(x_{L_1}, y_{L_2})$ ($N_2(x_{N_1}, y_{N_2})$) be the other intersection point between the orbit Γ_L (Γ_N) with the line $x = x_{L_1}$ ($x = x_{N_1}$). Then we have $y_{L_2} = y_{N_2}$.*

Proof. If we consider system S_1 in the phase space, then y can be seen as a function of x with the following differential equation

$$\frac{dy}{dx} = \frac{y}{x}\frac{\frac{cx}{1+\omega x} - qx - \delta}{r - py},$$

and integrating above equation from (x_1, y_1) to (x, y), one yields

$$\int_{x_1}^{x}\left(\frac{c}{1+\omega x} - q - \frac{\delta}{x}\right)dx = \int_{y_1}^{y}\left(\frac{r}{y} - p\right)dy.$$

Thus, the first integral $H_1(x, y)$ of system S_1 reads

$$H_1(x, y) = -\frac{c}{\omega}\ln(1+\omega x) + \delta\ln(x) + qx + r\ln(y) - py = h_1, \tag{12}$$

where $h_1 = H_1(x_1, y_1)$ is a constant.

Then, according to the definition of the Lambert W function and solving $H_1(x, y) = h_1$ with respect to y, one yields two roots

$$y_l^{S_1} = -\frac{r}{p}W\left[0, -\frac{p}{r}\exp\left(\frac{c\ln(1+\omega x) - \delta\omega\ln(x) - q\omega x + h_1\omega}{r\omega}\right)\right] \tag{13}$$

and

$$y_u^{S_1} = -\frac{r}{p}W\left[-1, -\frac{p}{r}\exp\left(\frac{c\ln(1+\omega x) - \delta\omega\ln(x) - q\omega x + h_1\omega}{r\omega}\right)\right]. \tag{14}$$

According to the Eq. (14) we can calculate that

$$y_{L_2} = -\frac{r}{p}W\left[-1, -\frac{p}{r}\exp \times\left(\frac{\rho\ln(1+\omega x_{L_1}) - \delta\omega\ln(x_{L_1}) - q\omega x_{L_1} + h_{11}\omega}{r\omega}\right)\right] \tag{15}$$

and

$$y_{N_2} = -\frac{r}{p}W\left[-1, -\frac{p}{r}\exp \times\left(\frac{\rho\ln(1+\omega x_{N_1}) - \delta\omega\ln(x_{N_1}) - q\omega x_{N_1} + h_{12}\omega}{r\omega}\right)\right], \tag{16}$$

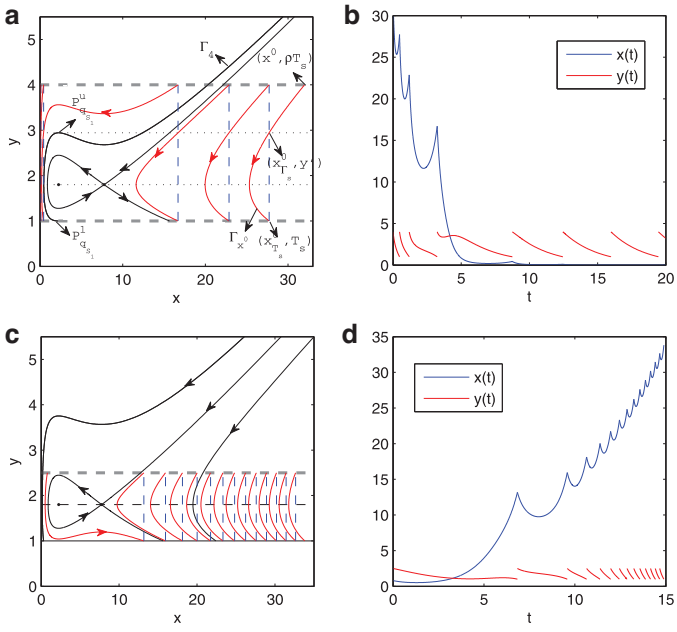

Fig. 2. (a) Dynamical behaviors of system (5) when $\rho T_s > y^u_{q_{S_1}}$ and (b) gives a few trajectories converging to the virus-free periodic solution $\zeta_{S_1}(t)$ under the above condition. (c) shows the dynamics of system (5) when $y^u_{S_1} < \rho T_s < y^u_{q_{S_1}}$ and (d) presents a few trajectories of which the horizontal components tend to infinity.

with $h_{11} = H_1(x_{L_1}, T_s)$ and $h_{12} = H_1(x_{N_1}, T_s)$. Through easy calculations we have

$$-\frac{p}{r}\exp\left(\frac{\rho\ln(1+\omega x_{L_1}) - \delta\omega\ln(x_{L_1}) - q\omega x_{L_1} + h_{11}\omega}{r\omega}\right) = -\frac{p}{r}\exp\left(\frac{\rho\ln(1+\omega x_{N_1}) - \delta\omega\ln(x_{N_1}) - q\omega x_{N_1} + h_{12}\omega}{r\omega}\right). \tag{17}$$

Then according to the properties of the Lambert W function, there is $y_{L_2} = y_{N_2}$. This completes the proof. □

To investigate the global dynamics of system (5) we just need to consider all the orbits starting from the region $D_I = \{(x, y) | y > T_s, x > 0\}$ because any given initial values of x and y can be changed to the region D_I after one time of impulsive immune therapy. For convenience, we denote the limit set $\overline{[T_s, \rho T_s]^\infty} = \{(x, y) | x = +\infty, T_s \le y \le \rho T_s\}$, which represents that the x component tends to infinity and the y component oscillates periodically with lower and upper bounded by T_s and ρT_s, respectively.

Theorem 2. *When $\rho T_s > y^u_{q_{S_1}}$, the virus-free periodic solution $\zeta_{S_1}(t)$ is stable in the region $D_I \setminus D_{\Gamma^1_{S_1}}$ while $E^1_{S_1}$ is stable in $D_{\Gamma^1_{S_1}}$ (as shown in Fig. 2(a and b)); If $y^u_{S_1} < \rho T_s < y^u_{q_{S_1}}$, then $\zeta_{S_1}(t)$ becomes unstable and $E^1_{S_1}$ is also stable in the region $D_{\Gamma^1_{S_1}}$ while all the other orbits starting from the region $D_I \setminus D_{\Gamma^1_{S_1}}$ will tend to $\overline{[T_s, \rho T_s]^\infty}$ (see Fig. 2(c and d)).*

Proof. The assumption $T_s < \min\{y^l_{S_1}, y^l_{S_2}\}$ guarantees that any orbit starting from the region $D_{\Gamma^1_{S_1}}$ will not approach the impulsive line $y = T_s$. Therefore, $E^1_{S_1}$ is always stable in the region $D_{\Gamma^1_{S_1}}$ according to the dynamics of system S_1. Let $(x^0, \rho T_s)$ be a point on the line $y = \rho T_s$. When $\rho T_s > y^u_{S_1}$, the orbit initiating from the point $(x^0, \rho T_s)$, denoted by Γ_{x^0}, will approach the line $y = T_s$ at finite time and we denote the intersection point of the line $y = T_s$ to the

orbit Γ_{x^0} as $(x^0_{T_s}, T_s)$ (shown in Fig. 2(a)). Then we can define the Poincaré map of system (5) as:

$$\Phi(x^0) = x^0_{T_s}.$$

We claim that $\Phi(x^0) - x^0 < 0$ when $\rho T_s > y^u_{q_{S_1}}$ and $\Phi(x^0) - x^0 > 0$ when $y^u_{S_1} < \rho T_s < y^u_{q_{S_1}}$. Without loss of generality, we just prove the case $\rho T_s > y^u_{q_{S_1}}$. Denote the intersection point of the orbit Γ^4 to the line $y = \rho T_s$ as $P_{\Gamma^4}(x_{\Gamma^4}, \rho T_s)$. We consider the two cases (a) $\{(x^0, y)|y = \rho T_s, 0 < x^0 < x^1_{S_1}$, or $x^0 > x_{\Gamma^4}\}$ and (b) $\{(x^0, y)|y = \rho T_s, x^1_{S_1} < x^0 < x_{\Gamma^4}\}$. For case (a), denote the intersection point of the orbit Γ_{x^0} to the line $x = x^0_{T_s}$ as $(x^0_{T_s}, y')$ (as shown in Fig. 2(a)). Then by Lemma 1, we have that $y' = y^u_{q_{S_1}} < \rho T_s$. Furthermore, when $0 < x < x^1_{S_1}$ or $x > x_{\Gamma^4}$, $y > y^1_{S_1}$ we have $dx/dt < 0$ and $dy/dt < 0$. Thus we have that $x^0_{T_s} < x^0$ (i.e. $\Phi(x^0) - x^0 < 0$). For case (b), all the orbits starting from it will approach the segment $\{(x, y)|y = T_s, 0 < x < x^1_{S_1}\}$. Therefore, there must be $\Phi(x^0) < x^0$ for $x^1_{S_1} < x^0 < x_{\Gamma^4}$ according to the definition of Φ.

Using the above properties of Φ, we can conclude that the trivial periodic solution $\zeta_{S_1}(t)$ is locally stable when $\rho T_s > y^u_{q_{S_1}}$ and unstable when $y^u_{S_1} < \rho T_s < y^u_{q_{S_1}}$. More specially, when $y^u_{S_1} < \rho T_s < y^u_{q_{S_1}}$ all the orbits initiating from the line $y = \rho T_s$ will tend to $\overline{[T_s, \rho T_s]^\infty}$ while all the orbits initiating from the line $y = \rho T_s$ tend to the virus-free periodic solution $\zeta_{S_1}(t)$ if $\rho T_s > y^u_{q_{S_1}}$. This completes the proof. □

Remark 1. In Theorem 2, there always exists a special case due to the stable one manifold of the equilibria $E^2_{S_1}$, that is, any orbit of system (5) approaching the intersection point of the orbit $\Gamma^2_{S_1}$ to the line $y = \rho T_s$ will finally tend to $E^2_{S_1}$. Therefore, when discuss the domain of attraction, we should get rid of the countable orbits.

Theorem 3. *If $y^l_{S_1} < \rho T_s < y^u_{S_1}$, then $\zeta_{S_1}(t)$ is unstable and $E^1_{S_1}$ is locally stable within the region $D_{\Gamma^1_{S_1}}$. The orbits starting from the region $D_I \setminus D_{\Gamma^1_{S_1}}$ either reach a periodic solution in the region $D_{\Gamma^1_{S_1}}$ or approach $\overline{[T_s, \rho T_s]^\infty}$, depending on initial values as shown in Fig. 3(a–c).*

Proof. When $y^l_{S_1} < \rho T_s < y^u_{S_1}$, there are two intersection points between the line $y = \rho T_s$ and the orbit $\Gamma^1_{S_1}$, which are denoted by $P^0_m(x^0_m, \rho T_s)$ and $P^0_n(x^0_n, \rho T_s)$ with $x^0_m < x^0_n$. The intersection point of the line $y = \rho T_s$ to the orbit Γ^4 is denoted by $P^0_l(x^0_l, \rho T_s)$ shown in Fig. 3(b and c). In this situation, the Poincaré map Φ can be well defined just when $0 < x^0 < x^0_m$ and $x^0 > x^0_n$ because all the orbits starting from the segment $\{(x, y)|y = \rho T_s, x^0_m < x < x^0_n\}$ are closed orbits within the domain $D_{\Gamma^1_{S_1}}$ which can not approach the line $y = T_s$ and hence free from impulsive immune therapy. Similar to the case $y^u_{S_1} < \rho T_s < y^u_{q_{S_1}}$, $\Phi(x^0) - x^0 > 0$ holds true for $x^0 \in (0, x^0_m)$ or $(x^0_n, +\infty)$. Thus, we have that $\zeta_{S_1}(t)$ is unstable and all the orbits of system (5) initiating from $\{(x, y)|y = \rho T_s, x > x^0_n\}$ will tend to $\overline{[T_s, \rho T_s]^\infty}$.

Let $P'^0_m = (x^0_m, T_s)$ and $P'^0_l = (x^0_l, T_s)$ with $x^0_l < x^0_m < x^1_{S_1}$ shown in Fig. 3(d). According to the dynamics of system S_1, the orbits passing through the points P'^0_m and P'^0_l will intersect with the line $y = \rho T_s$ at $P^1_m(x^1_m, \rho T_s)$ and $P^1_l(x^1_l, \rho T_s)$ respectively. Then let $P'^1_m(x^1_m, T_s)$ and $P'^1_l(x^1_l, T_s)$, and the intersection points of the line $y = \rho T_s$ with the orbits passing through the points P'^1_m and P'^1_l are denoted by $P^2_m(x^2_m, \rho T_s)$ and $P^2_l(x^2_l, \rho T_s)$ respectively. Repeating the above process, we can define the two sequences of points $\{P^n_m\}$ and $\{P^n_l\}$ (see Fig. 3(d)). From the definition of the Poincaré map Φ, we have $\Phi(x^{n+1}_m) = x^n_m$ and $\Phi(x^{n+1}_l) = x^n_l$. Further, there is $\Phi(x^0) - x^0 > 0, 0 < x^0 < x^0_m$, which means that $x^{n+1}_m < \Phi(x^{n+1}_m) = x^n_m$ and $x^{n+1}_l < \Phi(x^{n+1}_l) = x^n_l$. Then it follows from the existence and uniqueness of solutions of system S_1 that all the orbits initiating from the segment $\overline{P^{n+1}_l P^{n+1}_m}$ ($\overline{P^{n+2}_m P^{n+1}_l}$) will approach the segment $\overline{P^n_l P^n_m}$ ($\overline{P^{n+1}_m P^n_l}$) ($n = 0, 1, 2, \ldots$) after one time of impulsive therapy. Further, it follows from the dynamics of system (7) that all the orbits starting from $\overline{P^0_l P^0_m}$ will approach $\overline{P^{\Gamma^4}_{T_s} P^{\Gamma^3}_{T_s}}$, where $P^{\Gamma^4}_{T_s} = (x^{\Gamma^4}_{T_s}, T_s)$ and $P^{\Gamma^3}_{T_s} = (x^{\Gamma^3}_{T_s}, T_s)$ with $x^{\Gamma^3}_{T_s} > x^{\Gamma^4}_{T_s} > x^2_{S_1} > x^0_n$ are the intersection points of the line $y = T_s$ with the orbits Γ^4 and $\Gamma^3_{S_1}$ as shown in Fig. 1, and then tend to $\overline{[T_s, \rho T_s]^\infty}$ following the case $\{(x, y)|y = \rho T_s, x > x^0_n\}$. As a conclusion, all the orbits initiating from the segment $\overline{P^n_l P^n_m}$ will first approach $\overline{P^0_l P^0_m}$, and then tend to $\overline{[T_s, \rho T_s]^\infty}$. Whereas all the orbits initiating from $\overline{P^{n+1}_m P^n_l}$ initially reach $\overline{P^1_m P^0_l}$, and then approach the segment $\{(x, y)|y = \rho T_s, x^0_m < x < x^1_{S_1}\}$ while any orbit of system S_1 initiating from the segment $\{(x, y)|y = \rho T_s, x^0_m < x < x^1_{S_1}\}$ is a closed orbit. Denote the backward orbit of system S_1 initiating from the points P'^n_m and P'^n_l as $\Gamma_{P^{n+1}_m}$ and $\Gamma_{P^{n+1}_l}$ ($n = 0, 1, 2, \ldots$), and the domain bounded by the orbits $\Gamma_{P^n_m}$, $\Gamma_{P^n_l}$ ($\Gamma_{P^n_m}$, $\Gamma_{P^{n-1}_l}$) and the line $y = T_s$ is denoted by $D_{P^n_l P^n_m}$ ($D_{P^n_m P^{n-1}_l}$). Denote the region bounded by the orbits $\Gamma_{P^1_m}$, Γ^4 and the line $y = T_s$ as $D_{P^1_m P^0_l}$ and the region bounded by the orbit Γ^4, the curve $\Gamma^1_{S_1} \cup \Gamma^2_{S_1} \cup \Gamma^3_{S_1}$ and the line $y = T_s$ as $D_{P^0_l P^0_m}$. The domain bounded by the orbits $\Gamma^2_{S_1}$ and $\Gamma^3_{S_1}$ is denoted by $D_{\Gamma^2_{S_1}\Gamma^3_{S_1}}$. Therefore, any orbit starting from the domain $D_{P^{n+1}_m P^n_l}, n = 0, 1, 2, \ldots$ will approach a periodic solution and all the orbits initiating from the domain $D_{\Gamma^2_{S_1}\Gamma^3_{S_1}} \cup D_{P^n_l P^n_m} (n = 0, 1, 2, \ldots)$ will tend to $\overline{[T_s, \rho T_s]^\infty}$. This completes the proof. □

Corollary 1. *System (5) (or (6)) does not have positive order-k ($k = 1, 2, \ldots$) periodic solutions if $\rho T_s \neq y^u_{q_{S_1}}$ ($\rho T_s \neq y^u_{q_{S_2}}$), while for $\rho T_s = y^u_{q_{S_1}}$ (or $\rho T_s = y^u_{q_{S_2}}$) any solution of system (5) (or (6)) initiating from the line $y = \rho T_s$ ($y = \rho T_s$) except for the intersection point of the orbit $\Gamma^2_{S_1}$ ($\Gamma^2_{S_2}$) to the line $y = \rho T_s$ is a positive order-1 periodic solution.*

Remark 2. System (6) also has a virus-free periodic solution, denoted by $\zeta_{S_2}(t)$, which is stable when $\rho T_s > y^u_{q_{S_2}}$ and unstable when $y^l_{S_2} < \rho T_s < y^u_{q_{S_2}}$. And the results in Theorems 2 and 3 also hold true for system (6).

Remark 3. Comparing systems (5) and (6), we have that the continuous antiretroviral therapy and interleukin (IL)-2 treatment do not affect the dynamics of the virus-immune system with the impulsive immune therapy. However, there exist two lower critical values $y^u_{q_{S_1}}$ for system (5) and $y^u_{q_{S_2}}$ for system (6) with $y^u_{q_{S_2}} < y^u_{q_{S_1}}$ such that the corresponding virus-free periodic solutions is locally stable. That implies, with an additional continuous antiretroviral therapy and interleukin (IL)-2 treatment, the efficiency of immune therapy (ρ) can be relatively low to eradicate the virus (i.e. $y^u_{q_{S_2}} < \rho T_s < y^u_{q_{S_1}}$).

3.2. The dynamics of system (2) with only HIV-1 RNA-guided therapy considered

During therapy process for a HIV infected patient, if we don't consider the effector cell-guided impulsive immune therapy, then system (2) becomes the Filippov system (1). It is worth mentioning that when we consider the Filippov system (1), systems S_1 and S_2

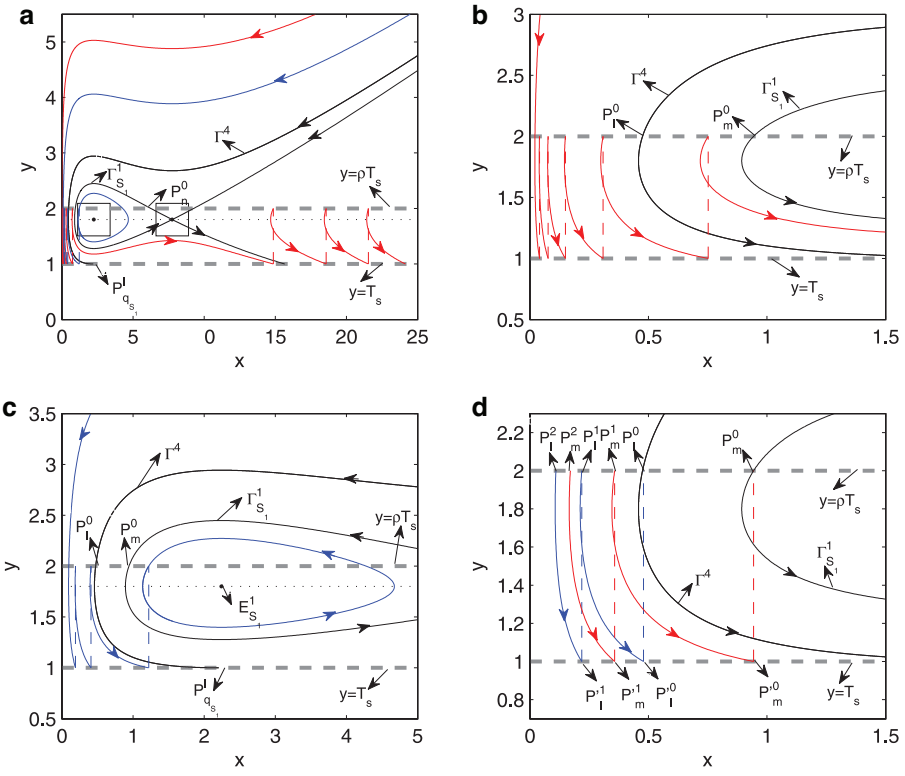

Fig. 3. (a) Dynamical behaviors of system (5) when $y^l_{S_1} < \rho T_s < y^u_{S_1}$; (b) is the partially enlarged drawing of (a) corresponding to the horizontal component of the orbits converging to infinity; (c) The partially enlarged drawing of (a) corresponding to the orbit reaching a closed orbit; (d) The schematic diagram of the definition of the point sequences of $\{P^n_m\}$ and $\{P^n_l\}$.

are defined as system S_1 in the regions $\{(x, y)|0 \le x < V_s, y \ge 0\}$ and system S_2 in $\{(x, y)|x > V_s, y \ge 0\}$ respectively.

The global dynamics of system (1) has been intensively discussed in the paper [17]. The main results showed that there are six scenarios for dynamical behaviors with different threshold values. These include that (a) equilibrium $E^1_{S_1}$ or $E^1_{S_2}$ is locally stable; (b) the pseudo-equilibrium E_c is locally stable; (c) a touching cycle and the equilibrium $E^1_{S_2}$ or $E^1_{S_1}$ are locally bistable; (d) equilibrium $E^1_{S_1}$ and the pseudo-equilibrium E_c are locally bistable. However, among all the cases $(0, +\infty)$ is also an attractor, depending on the initial conditions. This means that there always exists the situation that the virus will finally go to infinity whatever the threshold we choose. Interestingly, when we set $x^1_{S_2} < V_s < x^1_{S_1}$, the pseudo-equilibrium E_c is locally stable, and the controllable region, in which the virus can be controlled below a certain level and the effector cells can be maintain a certain level, can be maximized compared with other cases. Therefore, in this paper, we assume that $x^1_{S_2} < V_s < x^1_{S_1}$ always holds true.

To investigate the dynamics of system (1), there exists an important curve Y. When $x^1_{S_2} < V_s < x^1_{S_1}$, the line $x = V_s$ will intersect with the orbit $\Gamma^1_{S_2}$ at two points while the lower one is denoted by $P_3(V_s, y_3)$ as shown in Fig. 4. It follows from the dynamics of system S_1 that there exists an orbit Γ^5 initiating from P_3 intersecting the line $x = V_s$ at another point $P_4(V_s, y_4)$. Similarly, there must exist an orbit of system S_2 passing through the point P_4 and we denoted it as Γ^6. Then the curve Y can be defined as $\Gamma^6 \cup \widehat{P_4P_3} \cup \widehat{P_3E^2_{S_2}} \cup \Gamma^2_{S_2}$ and the region inside the curve Y is denoted by D_Υ. Then the dynamic of system (1) when $x^1_{S_2} < V_s < x^1_{S_1}$ can be described as follows for a detail proof, see [17].

Theorem 4. *When $x^1_{S_2} < V_s < x^1_{S_1}$, there exists a pseudo-equilibrium E_c of system (1) which is locally asymptotically stable in D_Υ; Any orbit initiating from $R^2_+ \setminus D_\Upsilon$ tends to $(\infty, 0)$ (see Fig. 4).*

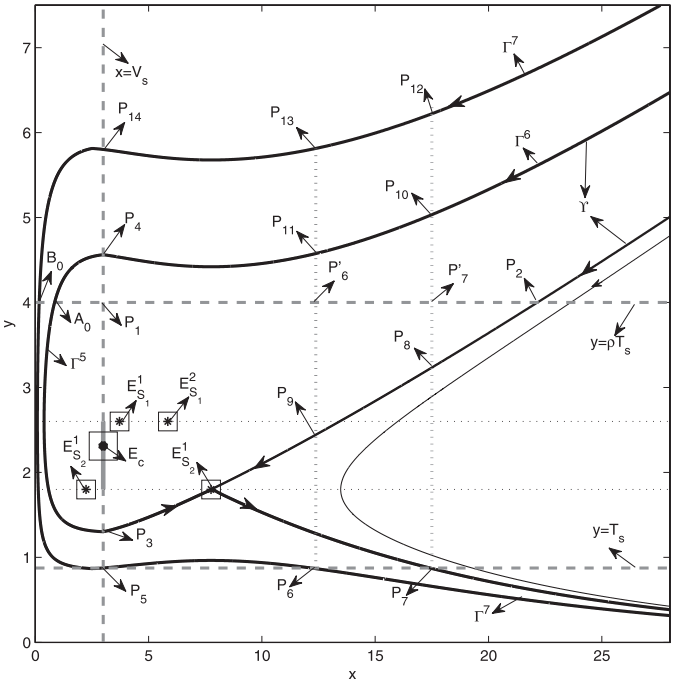

Fig. 4. The topological structure of the Filippov system (1) when $x^1_{S_2} < V_s < x^1_{S_1}$. All the parameter values are fixed as $r = 2.6, p = 1, c = 0.5, q = 0.23, \delta = 0.5, \omega = 0.5, \epsilon_1 = 0.2, \epsilon_2 = 0.8, V_s = 3$.

To discuss the global dynamics of system (2), we define several critical points as follows (see Fig. 4). The intersection point between the two lines $x = V_s$ and $y = \rho T_s$ is denoted by $P_1(V_s, \rho T_s)$. When $\rho T_s > y^2_{S_2}$, then the line $y = \rho T_s$ will intersect with the

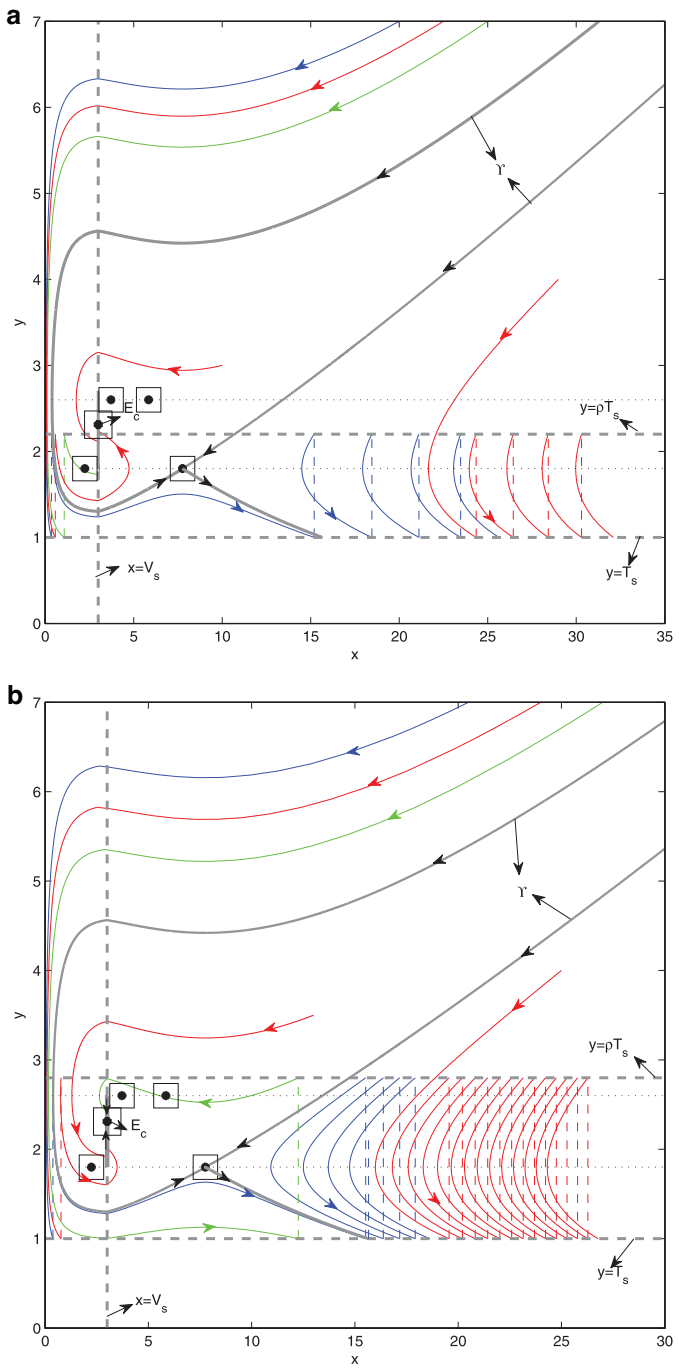

Fig. 5. (a) Dynamical behaviors of system (2) when $y^2_{S_2} < \rho T_s < y_9$ with $\rho = 2.2$. (b) Dynamical behaviors of system (2) when $y_9 < \rho T_s < y_8$ with $\rho = 2.8$. The other parameter values are: $r = 2.6, p = 1, c = 0.5, q = 0.23, \delta = 0.5, \omega = 0.5, \epsilon_1 = 0.2, \epsilon_2 = 0.8, V_s = 3, T_s = 1$.

orbit $\Gamma^2_{S_2}$ at $P_2(x_2, \rho T_s)$. Let $P_5 = (V_s, T_s)$ and we denote the orbit of the Filippov system (1) passing through P_5 as Γ^7 and the other intersection point of the line $y = T_s$ with the orbit Γ^7 as P_6. The intersection point of the orbit $\Gamma^3_{S_2}$ with the line $y = T_s$ is denoted by $P_7(x_7, y_7)$. Also we denote the intersection point between the two lines $x = x_6$ $(x = x_7)$ and $y = \rho T_s$ by $P'_6(x_6, \rho T_s)$ $(P'_7(x_7, \rho T_s))$. Denote the intersection points of the line $x = x_7$ $(x = x_6)$ with the orbit $\Gamma^2_{S_2}$ as $P_8(x_8, y_8)$ $(P_9(x_9, y_9))$, with the orbit Γ^6 as $P_{10}(x_{10}, y_{10})$ $(P_{11}(x_{11}, y_{11}))$ and with the orbit Γ^7 as $P_{12}(x_{12}, y_{12})$ $(P_{13}(x_{13}, y_{13}))$. Let $P_{14}(x_{14}, y_{14})$ be the other intersection point of the orbit Γ^7 with the line $x = V_s$. we can easily get the following relationship $y_5 = y_6 = y_7 < y_3 < y^2_{S_2} < y_9 < y_8$, $y_{11} < y_{10}$ and $y_{13} < y_{12}$. It follows from Lemma 2 in Appendix that $y_{14} = y_{13}$ and $y_4 = y_{11}$. According to Lemmas 1 and 2 in Appendix, we have that $y^u_{q_{S_1}} = y_{14}$ and $y^u_{q_{S_2}} = y_8$ with $y^u_{q_{S_1}} > y^u_{q_{S_2}}$. It follows from Lemma 2 that if we fix all the other parameter values, then x_6 keeps constant as T_s decreases, which also means that y_9 and y_{11} will not change as T_s changes. Further, it follows from Lemma 3 that $y_9 < y_4$ always holds true. The definitions of the points P_8, P_{10} and P_{12} show us that y_8, y_{10} and y_{11} are strictly increasing to $+\infty$ with $y_8 < y_{10} < y_{12}$ as T_s decreases to 0, thus the relationship between y_8 and y_{11} cannot be determinated. Due to the complexity of the Filippov system (1), it is difficult to theoretically analyze the relationship of y_{10} and y_{13}. Numerical results show that it can happen that $y_{10} < y_{13}$ and P_8 is below the minimum point of the orbit Γ^6 (i.e. the intersection point of the line $x = x^2_{S_2}$ to the orbit Γ^6, denoted by $P_{15}(x^2_{S_2}, y_{15})$). In the following, we assume $y_{10} < y_{13}$. Therefore, if we let the value of threshold T_s change and fix all the other parameter values, we have case $\mathcal{C}1 : y_3 < y^2_{S_2} < y_9 < y_{15} < y_4 = y_{11} < y_{10} < y_{13} = y_{14} = y^u_{q_{S_1}} < y_{12}$ or case $\mathcal{C}2 : y_3 < y^2_{S_2} < y_{15} < y_9 < y_4 = y_{11} < y_{10} < y_{13} = y_{14} = y^u_{q_{S_1}} < y_{12}$. In case $\mathcal{C}1$ three subcases are possible:

$$\mathcal{C}11 : y_9 < y_8 = y^u_{q_{S_2}} < y_{15}; \quad \mathcal{C}12 : y_{15} < y_8 = y^u_{q_{S_2}} < y_{11};$$
$$\mathcal{C}13 : y_{11} < y_8 = y^u_{q_{S_2}} < y_{10}.$$

while in case $\mathcal{C}2$ two subcases are possible:

$$\mathcal{C}21 : y_9 < y_8 = y^u_{q_{S_2}} < y_{11}; \quad \mathcal{C}22 : y_{11} < y_8 = y^u_{q_{S_2}} < y_{10}.$$

In the next section we mainly consider the global dynamics of system (2) for case $\mathcal{C}11$ while for the other cases the discussion for the dynamics are similar.

4. The global dynamics of system (2)

In this section, we will investigate the global dynamics of system (2). Denote the region bounded by $\widehat{P_5P_6}$ and $y = T_s$ as $D_{P_5P_6}$ and let $D_{I'} = D_I \setminus D_{P_5P_6}$. Then we only need to consider all the orbits initiating from the region $D_{I'}$ when $\rho T_s > y_3$ since orbits initiating from the region $R^2_+ \setminus D_{I'}$ can jump into $D_{I'}$ after an impulsive immune therapy. Note that the assumption $T_s < \min\{y^I_{S_1}, y^I_{S_2}\}$ guarantees that all the orbits of system (2) initiating from the domain D_Υ cannot approach the line $y = T_s$, that is, impulsive immune therapy will not happen. Therefore, it follows from the dynamics of the Filippov system (1) that the pseudo-equilibrium E_c is always stable within the domain D_Υ whatever the value of ρT_s is. At the same time, any orbit in the domain $D_{I'} \setminus D_\Upsilon$ can pass through the line $y = \rho T_s$, which means that we just need to consider all the orbits initiating from the line $y = \rho T_s$. When $y_3 < \rho T_s < y_4$, there is an intersection point between the line $y = \rho T_s$ and the orbit Γ^5, denoted by $A_0(x_{A_0}, \rho T_s)$ and the intersection point of the line $y = \rho T_s$ with the orbit Γ^7 is denoted as $B_0(x_{B_0}, \rho T_s)$ when $y_5 < \rho T_s < y_{14}$ as shown in Fig. 4.

As mentioned in the previous section, we assume that $x^1_{S_2} < V_s < x^1_{S_1}$ and $T_s < \min\{y^I_{S_1}, y^I_{S_2}\}$ always hold true with case $\mathcal{C}11$ in the rest of this paper. Therefore, the key factor determining the dynamics of system (2) is the level of the intensity of immune therapy ρ under these assumptions. In the following we consider several scenarios in terms of relation of ρT_s and $y_3, y^2_{S_2}, y_9, y_8, y_{11}, y_{10}, y_{13}, y_{12}$.

Firstly, let $y_3 < \rho T_s \le y_9$ hold true. Here we initially consider the case of $y^2_{S_2} < \rho T_s < y_9$ as an illustration. In a such case, the line $y = \rho T_s$ is divided by orbit Y into three parts: $\{(x, y)|x > x_2, y = \rho T_s\}$, $\{(x, y)|x_{A_0} < x < x_2, y = \rho T_s\}$ and $\{(x, y)|0 < x < x_{A_0}, y = \rho T_s\}$.

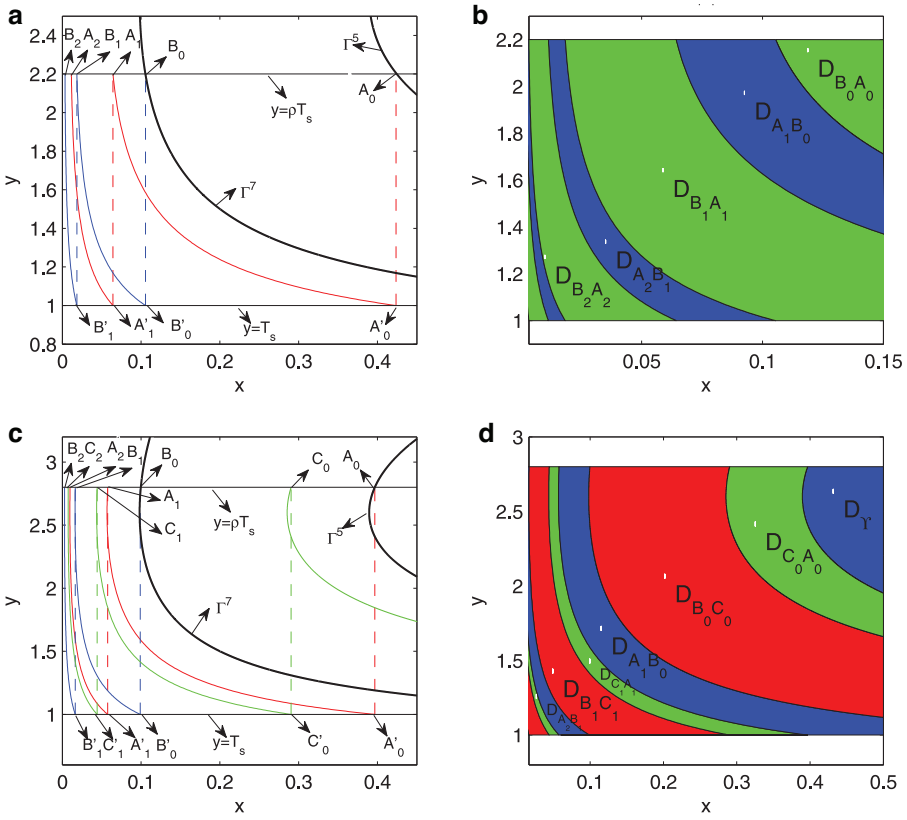

Fig. 6. (a) Schematic diagram of the definitions of the point sequences of $\{A_n\}$ and $\{B_n\}$, (b) The basin of attraction domain of system (2) when $y^2_{S_2} < \rho T_s < y_9$; (c) Schematic diagram of the definitions of $\{A_n\}$, $\{B_n\}$ and $\{C_n\}$, (d) The basin of attraction domain of system (2) when $y_9 < \rho T_s < y_8$.

It is easy to see that any orbit initiating from segment $\{(x,y)|x_{A_0} < x < x_2, y = \rho T_s\}$ will finally tend to the pseudo-equilibrium E_c since it belongs to the domain D_Υ.

Within the domain bounded by the orbits $\Gamma^2_{S_2}$ and $\Gamma^3_{S_2}$, all the orbits initiating from the segment $\{(x,y)|x > x_2, y = \rho T_s\}$ can not approach the switching line $x = V_s$, which means that the dynamics will just follow the system S_2 with impulsive immune therapy (i.e. system (6)). Furthermore, when $\rho T_s < y_9$, according to the proof of Theorem 2, we have that $\Phi(x^0) - x^0 > 0$ holds true, where Φ is the Poincaré map of system (6). Therefore, we can conclude that all the orbits starting from $\{(x,y)|x_2 < x, y = \rho T_s\}$ will tend to $\overline{[T_s, \rho T_s]^\infty}$ (see Fig. 5(a)).

Before discussing the asymptomatic behaviors of solution starting from the segment $\{(x,y)|0 < x < x_{A_0}, y = \rho T_s\}$, we initially define two sequences of points. Let $A'_0 = (x_{A_0}, T_s)$ and $B'_0 = (x_{B_0}, T_s)$ shown in Fig. 6(a). It follows from the dynamics of system S_1 that the orbit initiating from the point A'_0 will intersect with the line $y = \rho T_s$ at $A_1(x_{A_1}, \rho T_s)$ and let $A'_1 = (x_{A_1}, T_s)$. Similarly we denote the intersection point of the line $y = \rho T_s$ with the orbit of system S_1 passing through the point A'_1 as $A_2(x_{A_2}, \rho T_s)$. Repeating the above process, we can define two sequences of points $\{A_n\}$ on the line $y = \rho T_s$ and $\{A'_n\}$ on the line $y = T_s$ as shown in Fig. 6(a). Through the same process, we can also define the two sequences of points $\{B_n\}$ and $\{B'_n\}$. From the definitions of $\{A_n\}$ and $\{B_n\}$, there are $\Phi(x_{A_{n+1}}) = x_{A_n}$ and $\Phi(x_{A_{n+1}}) = x_{A_n}$ $(n = 0, 1, 2, \ldots)$, where Φ is the Poincaré map of system (5). When $\rho T_s < y_9 < y^u_{q_{S_1}}$, $\Phi(x^0) - x^0 > 0$ holds true, which means that $x_{A_{n+1}} < \Phi(x_{A_{n+1}}) = x_{A_n}$ and $x_{B_{n+1}} < \Phi(x_{B_{n+1}}) = x_{B_n}$. Further, note that $x_{A_0} > x_{B_0}$, we then conclude

$$x_{A_0} > x_{B_0} > x_{A_1} > x_{B_1} > \cdots > x_{A_n} > x_{B_n} > \cdots.$$

According to the existence and uniqueness of solutions of system S_1, any orbit initiating from the segment $\overline{B_nA_n}$ $(\overline{A_{n+1}B_n})$ will approach $\overline{B'_{n-1}A'_{n-1}}$ $(\overline{A'_nB'_{n-1}})$, and then jump to $\overline{B_{n-1}A_{n-1}}$ $(\overline{A_nB_{n-1}})$ with one time of impulsive immune therapy. Further, it follows from the dynamics of the Filippov system (1) that all the orbits of system (2) starting from the segment $\overline{B_0A_0}$ will reach $\overline{P_6P_7}$, followed with impulsive immune therapy and jump to $\overline{P'_6P'_7}$, and finally tend to $\overline{[T_s, \rho T_s]^\infty}$ following the case $\{(x,y)|y = \rho T_s, x > x_2\}$ because $x_6 > x_2$ in this situation. Meanwhile, it follows from the definition of A_1 and B_0 that any orbit initiating from the segment $\overline{A_1B_0}$ will reach $\overline{A'_0P_5}$, jumps to the segment $\overline{A_0P_1} \in D_\Upsilon$ and then tend to E_c. Therefore, we can conclude that

$$\cdots \to \overline{A_{n+1}B_n} \to \overline{A_nB_{n-1}} \to \cdots \to \overline{A_1B_0} \to \overline{A_0P_1} \to E_c,$$

$$\cdots \to \overline{B_nA_n} \to \overline{B_{n-1}A_{n-1}} \to \cdots \to \overline{B_0A_0} \to \overline{P'_6P'_7} \to (+\infty, \rho T_s),$$

where $\overline{A_{n+1}B_n} \to \overline{A_nB_{n-1}}$ represents that all the orbits starting from the segment $\overline{A_{n+1}B_n}$ will reach the segment $\overline{A_nB_{n-1}}$ after one time of impulsive immune therapy, and other notations should be interpreted similarly.

We denote the domain, bounded by the orbit Γ^7, the curve $\Gamma^6 \cup \widehat{P_4P_3} \cup \widehat{P_3E^2_{S_2}} \cup \Gamma^3_{S_2}$ and the line $y = T_s$ by $D_{B_0A_0}$. The negative orbits of Filippov system (1) initiating $\{A'_{n-1}\}$ and $\{B'_{n-1}\}$ $(n = 1, 2, \ldots)$ are denoted as Γ_{A_n} and Γ_{B_n} respectively, and the domains bounded by Γ_{B_n}, Γ_{A_n} $(\Gamma_{B_n}, \Gamma_{A_{n+1}})$ and line $y = T_s$ are denoted by $D_{B_nA_n}$ $(D_{A_{n+1}B_n})$. Especially, the domain bounded by the orbits Γ_{A_1}, Γ^7 and the line $y = T_s$ is denoted by $D_{A_1B_0}$. We also denote the region bounded by $\Gamma^2_{S_2}$, $\Gamma^3_{S_2}$ and the line $y = T_s$ by $D_{\Gamma^{23}}$. When $y_3 < y \le y^2_{S_2}$, the dynamics is same as the case $y^2_{S_2} < y < y_9$. Therefore, the global dynamics of system (2) when $y_3 < \rho T_s < y_9$ can be concluded as follows.

Theorem 5. *When $y_3 < \rho T_s < y_9$, then the pseudo-equilibrium E_c is stable in the basin of attraction region $D_{A_{n+1}B_n}(n = 0, 1, 2, \ldots) \cup D_\Upsilon$ while all orbits starting from the region $D_{B_nA_n}(n = 0, 1, 2, \ldots) \cup D_{\Gamma^{23}}$ will tend to $\overline{[T_s, \rho T_s]}^\infty$ (see Figs. 5(a) and 6(b)).*

If $y_9 < \rho T_s < y_8$, the dynamics of system (2) on the segments $\{(x, y)|x > x_2, y = \rho T_s\}$ and $\{(x, y)|x_{A_0} < x < x_2, y = \rho T_s\}$ are similar to those for the case $y_3 < \rho T_s < y_9$, hence here we omit it. For the rest part $\{(x, y)|0 < x < x_{A_0}, y = \rho T_s\}$, another sequence of points should be defined.

Let $P_2' = (x_2, T_s)$, and the orbit of Filippov system (1) passing through the point P_2' intersects the line $y = \rho T_s$ at $C_0 = (x_{C_0}, \rho T_s)$. Denote $C_0' = (x_{C_0}, T_s)$ and the orbit of system S_1 passing through the point C_0' intersects the line $y = \rho T_s$ at $C_1 = (x_{C_1}, \rho T_s)$. Similarly, let $C_1' = (x_{C_1}, T_s)$. Repeating the above process we can define the sequences $\{C_n\}$ on the line $y = \rho T_s$ and $\{C_n'\}$ on the line $y = T_s$ as shown in Fig. 6(c). Therefore, we have that all the orbits initiating from the segment $\overline{A_nB_{n-1}}$ ($\overline{B_nC_n}$, $\overline{C_nA_n}$) will reach the segment $\overline{A_{n-1}B_{n-2}}$ ($\overline{B_{n-1}C_{n-1}}$, $\overline{C_{n-1}A_{n-1}}$) after one impulsive effect. Furthermore, the orbits starting from $\overline{B_0C_0}$ (or $\overline{A_1B_0}$) will first approach the segment $\overline{P_6'P_2}$ (or $\overline{A_0P_1}$), and then tend to the pseudo-equilibrium E_c along the Filippov system (1). Similarly, the orbits initiating from the segment $\overline{C_0A_0}$ will first approach the segment $\overline{P_2P_7'}$, and then tend to infinity along the system S_2 with impulsive. As a conclusion, we have

$$\cdots \to \overline{B_nC_n} \to \overline{B_{n-1}C_{n-1}} \to \cdots \to \overline{B_0C_0} \to \overline{P_6'P_2} \to E_c,$$

$$\cdots \to \overline{A_{n+1}B_n} \to \overline{A_nB_{n-1}} \to \cdots \to \overline{A_1B_0} \to \overline{A_0P_1} \to E_c,$$

$$\cdots \to \overline{C_nA_n} \to \overline{C_{n-1}A_{n-1}} \to \cdots \to \overline{C_0A_0} \to \overline{P_2P_7'} \to (+\infty, \rho T_s).$$

Denote the backward orbits of the Filippov system (1) initiating from C_n' as Γ_{C_n}, and the region bounded by Γ_{C_n}, Γ_{B_n} (Γ_{C_n}, Γ_{A_n}) and $y = T_s$ as $D_{B_nC_n}$ ($D_{C_nA_n}$). The domain $D_{B_0A_0}$ is divided by the orbit of Filippov system (1) passing through the point C_0 into two subregions with the left part denoted by $D_{B_0C_0}$ and the right part denoted by $D_{C_0A_0}$. The dynamics of system (2) when $y_9 < \rho T_s < y_8$ is concluded as the follows.

Theorem 6. *When $y_9 < \rho T_s < y_8$, then the pseudo-equilibrium E_c is locally stable in the basin of attraction domain $D_\Upsilon \cup D_{B_nC_n} \cup D_{A_{n+1}B_n}(n = 0, 1, 2, \ldots)$. The orbits initiating from the region $D_{\Gamma^{23}} \cup D_{C_nA_n}(n = 0, 1, 2, \ldots)$ will tend to $\overline{[T_s, \rho T_s]}^\infty$, as shown in Figs. 5(b) and 6(d).*

For $y_8 < \rho T_s < y_{11}$, the whole segment $P_6'P_7'$ is contained in the domain D_Υ. For the case $\{(x, y)|x_2 < x, y = \rho T_s\}$, when $\rho T_S > y_8$, it follows from the system S_2 with pulse that the Poincaré map Φ of system (6) is strictly decreasing, which means that all the orbits starting from it will finally arrive at the segment $\overline{P_7'P_2}$, and then tend to the pseudo-equilibrium E_c following the dynamics of Filippov system (1).

For the orbits initiating from the segment $\{(x, y)|0 < x < x_{A_0}, y = \rho T_s\}$, it is similar to the case $y_{S_2}^2 < \rho T_s < y_8$. That is, the orbits initiating from the segment $\overline{A_nB_{n-1}}$ will first reach the segment $\overline{A_0P_1}$ after n times impulsive effects, and then tend to E_c along the dynamics of Filippov system (1). Any orbit initiating from the segment $\overline{B_nA_n}$ firstly reaches $\overline{B_0A_0}$, tends to $\overline{P_6P_7}$ following the Filippov system (1), then jumps to the segment $\overline{P_6'P_7'}$, and finally tends to the pseudo-equilibrium E_c along the Filippov system (1) as shown in Fig. 7.

Considering the case $\{(x, y)|x_{A_0} < x < x_2, y = T_s\}$, if line $y = \rho T_s$ doesn't intersect with the orbit Γ^6, we have the whole segment $\overline{A_0P_2}$ belongs to the region D_Υ, then it follows from the Filippov system that any orbit starting from it will directly tend to the pseudo-equilibrium E_c. If line $y = \rho T_s$ does intersect with the orbit

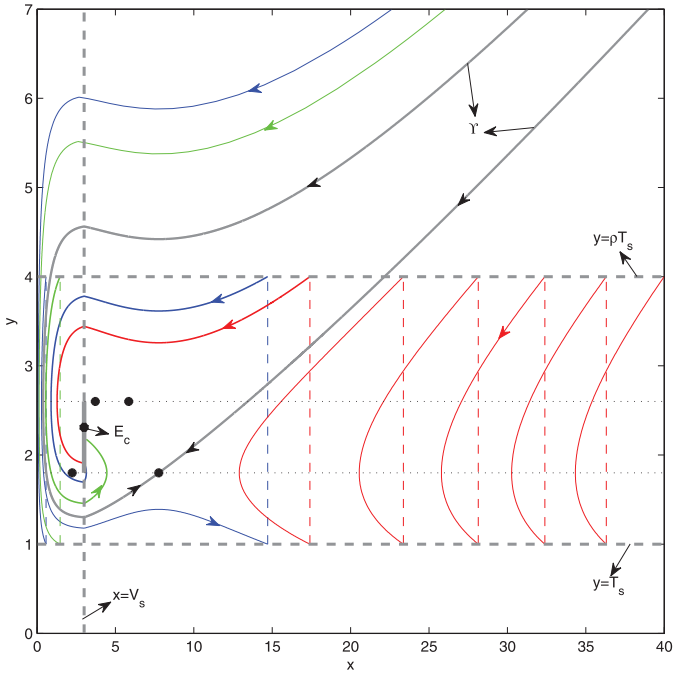

Fig. 7. The case that the pseudo-equilibrium E_c is globally stable when $y_8 < \rho T_s < y_{11}$ with $\rho = 4$. The other parameters are fixed as these in Fig. 5(a).

Γ^6, the segment $\overline{A_0P_2}$ is delivered into two parts. Then orbits starting from the part inside the domain D_Υ will directly tend to E_c as well, while orbits initiating from the part outside the domain D_Υ will first arrive at the segment $P_6'P_7'$, and then tend to E_c according to the case $\{(x, y)|0 < x < x_{A_0}, y = \rho T_s\}$. Therefore, when $y_8 < \rho T_s < y_{11}$, the dynamics of system (2) is as follows.

Theorem 7. *When $y_8 < \rho T_s < y_{11}$, then the pseudo-equilibrium E_c is globally stable as shown in Fig. 7.*

If $y_{10} < \rho T_s < y_{13}$, then $\rho T_s > y_{11}$ holds true. Therefore, there exists one and only one intersection point of the line $y = \rho T_s$ with the orbit Γ^6, denoted by $P_{16}(x_{16}, \rho T_s)$ shown in Fig. 8(b). We mainly consider the orbits initiating from the segments $\{(x, y)|0 < x < x_{B_0}, y = \rho T_s\}$, $\overline{B_0P_{16}}$ and $\{(x, y)|x > x_2, y = \rho T_s\}$ because the orbits starting from the segment $\overline{P_{16}P_2}$ will directly tend to the pseudo-equilibrium E_c following the dynamics of the Filippov system (1).

First of all, we consider the orbits initiating from the segment $\overline{P_6'P_7'}$ which is now out of the region D_Υ. The definition of the Poincaré map of system (2) on segment $\overline{P_6'P_7'}$ is similar to the definition of the Poincaré map of system (5), hence for convenience we also denote the Poincaré map of system (2) as Φ. That is, for $(x^0, \rho T_s)$, $x^0 \in (x_6, x_7)$, the orbit of the Filippov system (1) initiating from it will intersect with the line $y = T_s$ at (x_1^0, T_s), then we have $\Phi(x^0) = x_1^0$. When $y_{10} < \rho T_s < y_{13}$, it follows from the existence and uniqueness of solutions and the continuous dependence of the solution on the initial value of the systems S_1 and S_2 that Φ is continuous with $\Phi(x_6) - x_6 > 0$ and $\Phi(x_7) - x_7 < 0$. Therefore, the Poincaré map Φ has a fixed point in the interval (x_6, x_7), correspondingly the system (2) exists a positive order-1 periodic solution as shown in Fig. 8(c). However, it is difficult to prove the monotonicity of the function $\Phi(x^0) - x^0, x^0 \in (x_6, x_7)$ due to the complexity of the Poincaré map Φ. The numerical result (see Fig. 8(a)) shows that the map $\Phi(x^0) - x^0, x^0 \in (x_6, x_7)$ is strictly monotonically decreasing in the interval (x_6, x_7) when $y_{10} < \rho T_s < y_{13}$. Thus, when $\Phi(x^0) - x^0, x^0 \in (x_6, x_7)$ is strictly monotonically decreasing, then there exists one and only one fixed

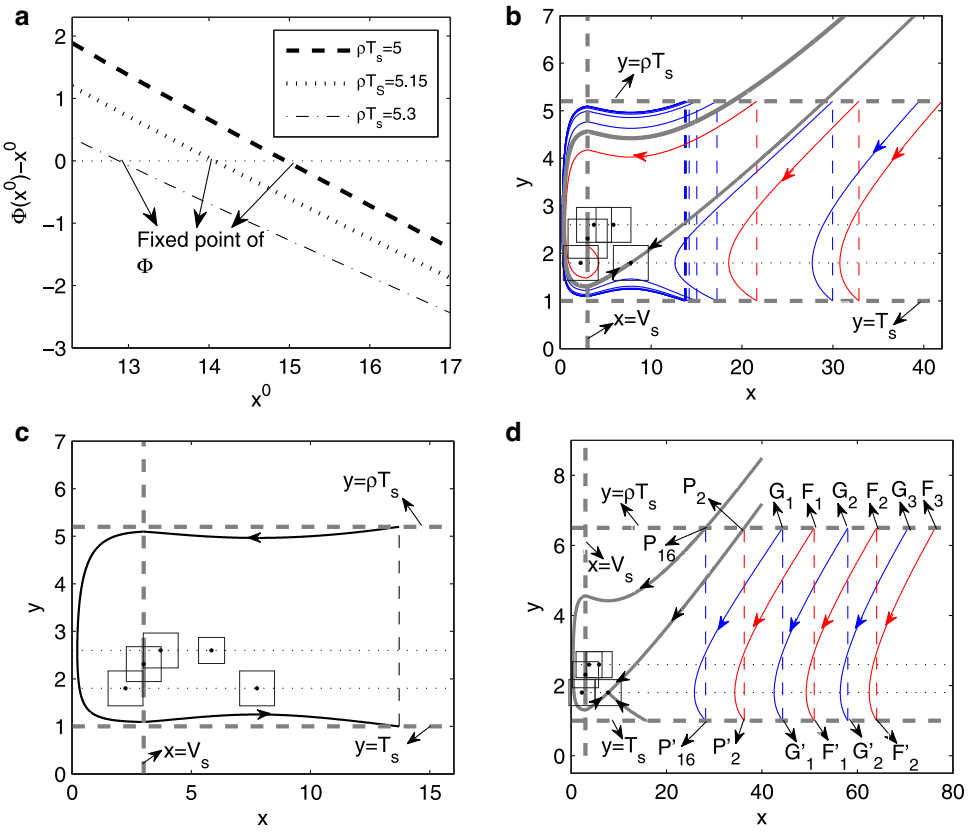

Fig. 8. (a) The curves of the map $\Phi(x^0)-x^0, x^0\in(x_6,x_7)$ when $y_{10}<\rho T_s<y_{13}$. (b) Dynamical behaviors of system (2) when $y_{10}<\rho T_s<y_{13}$. (c) shows the existence of the positive order-1 periodic solution $\Theta(t)$. (d) The schematic diagram of the definition of sequences of $\{G_n\}$ and $\{F_n\}$.

point of Φ, correspondingly, system (2) has one and only one positive periodic solution, denoted by $\Theta(t)$ (see Fig. 8(c)). Simultaneously, the monotonicity of the function $\Phi(x^0)-x^0$ also implies that the positive periodic solution $\Theta(t)$ is locally stable. Then we can conclude that any orbit starting from the segment $\overline{B_0P_{16}}$ will finally tend to $\Theta(t)$ since it will approach $\overline{P_6P_7}$ and jump into $\overline{P_6'P_7'}$.

It follows from the system S_1 with pulse (i.e. system (5)) that all the orbits initiating from the segment $\{(x,y)|0<x<x_{B_0}, y=\rho T_s\}$ will first reach the segment $\overline{B_0P_1}$, and then tend to the positive order-1 periodic solution $\Theta(t)$ following the former case.

Let $P'_{16}=(x_{16},T_s)$ and $P'_2=(x_2,T_s)$. Denote the intersection points of the line $y=\rho T_s$ with the orbit of system S_2 passing through the points P'_{16} and P'_2 as $G_1(x_{G_1},\rho T_s)$ and $F_1(x_{F_1},\rho T_s)$, respectively. Then let $G'_1=(x_{G_1},T_s)$ and $F'_1=(x_{F_1},T_s)$. Similarly, the intersection point between the line $y=\rho T_s$ and the orbit of system S_2 passing through the point G'_1 (F'_1) is denoted by $G_2(x_{G_2},\rho T_s)$ ($F_2(x_{F_2},\rho T_s)$). Repeating the above process we can define the sequences $\{F_n\}$ and $\{G_n\}$ with $n=1,2,\ldots,$ as shown in Fig. 8(d). From the definition of $\{F_n\}$ and $\{G_n\}$, we have that

$$x_{G_1}<x_{F_1}<x_{G_2}<x_{F_2}<\cdots<x_{G_n}<x_{F_n}<\cdots. \tag{18}$$

Then according to the existence and uniqueness of solutions and the dynamics of system (8), we have that any orbit starting from the segment $\overline{G_nF_n}$ will reach the segment $\overline{G_{n-1}F_{n-1}}$ after one impulsive effect while other orbits starting from the segment $\overline{F_{n-1}G_n}$ will reach the segment $\overline{F_{n-2}G_{n-1}}$. Note that the orbits initiating from the segment $\overline{G_1F_1}$ ($\overline{P_2G_1}$) will arrive at $\overline{P_{16}P_2}$ ($\overline{P'_7P_{16}}$). As a conclusion, we have

$$\cdots\to\overline{F_{n-1}G_n}\to\overline{F_{n-2}G_{n-1}}\to\cdots\to\overline{P_2G_1}\to\overline{P'_7P_{16}}\to\Theta(t),$$

and

$$\cdots\to\overline{G_nF_n}\to\overline{G_{n-1}F_{n-1}}\to\cdots\to\overline{G_1F_1}\to\overline{P_{16}P_2}\to E_c.$$

The orbits of system S_2 passing through the points $\{F_n\}$ and $\{G_n\}$ are denoted by Γ_{F_n} and Γ_{G_n}, respectively. Denote the domain bounded by the curve $\Gamma^6\cup\Gamma^5\cup\widehat{P_3E^2_{S_2}}\cup\Gamma^3_{S_2}$, the lines $y=T_s$ and $x=0$ as $D_{P'_{16}}$, the region bounded by Γ_{G_n}, Γ_{F_n} and $y=T_s$ as $D_{G_nF_n}$ $(n=1,2,\ldots)$, the region bounded by Γ_{F_n}, $\Gamma_{G_{n+1}}$ and $y=T_s$ as $\Gamma_{F_nG_{n+1}}$ $(n=2,3,\ldots)$. The region bounded by Γ_{G_1}, $\Gamma^2_{S_2}$, $\Gamma^3_{S_2}$ and $y=T_s$ is denoted by $D_{P_2G_1}$. Thus, the dynamics of system (2) for $y_{10}<\rho T_s<y_{13}$ can be concluded as follows.

Theorem 8. *When $y_{10}<\rho T_s<y_{13}$, then system (2) has a positive order-1 periodic solution $\Theta(t)$. Further, if $\Phi(x^0)-x^0$ is strictly monotonically decreasing, $\Theta(t)$ and E_c are bistable in the basin of attraction region $D_{P'_{16}}\cup D_{P_2G_1}\cup D_{F_nG_{n+1}}$ and $D_\Upsilon\cup D_{G_nF_n}$ $(n=1,2,\ldots)$, respectively.*

If $\rho T_s>y_{12}$, we have $\rho T_s>y_{12}>y_{13}=y_{14}=y^u_{q_{S_1}}$, and then there is one and only one intersection point of the line $y=\rho T_s$ to the orbit Γ^7 denoted by $P_{17}(x_{17},\rho T_s)$. It follows from the system S_1 with pulse that all the orbits initiating from the segment $\{(x,y)|0<x<x_{17}, y=\rho T_s\}$ will finally tend to the virus-free periodic solution $\zeta_{S_1}(t)$. Any orbit starting from the segment $\overline{P_{17}P_{16}}$ will first reach the segment $\overline{P_6P_7}$, jump to the segment $\overline{P'_6P'_7}$ with one impulsive effect, and finally tend to the the virus-free periodic solution because of $0<x_6<x_7<x_{17}$. Note that the orbits starting from the segment $\overline{P_{16}P_2}$ can not approach the line $y=T_s$, and therefore finally must tend to E_c along the Filippov system (1).

For the segment $\{(x,y)|x>x_2, y=\rho T_s\}$, the definitions of $\{F_n\}$ and $\{G_n\}$ are same as those for the case $y_{10}<\rho T_s<y_{13}$ (shown in

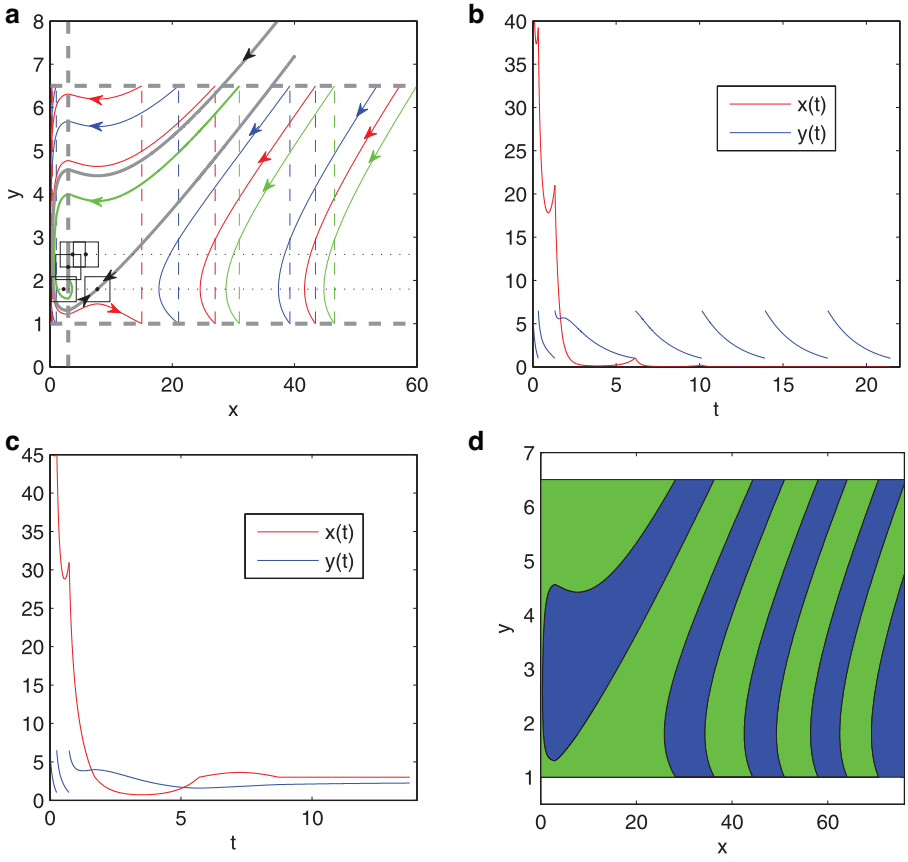

Fig. 9. (a)Dynamical behaviors of system (2) when $\rho T_s > y_{12}$ with $\rho = 6.5$. (b) and (c) show that the solution trajectories tent to E_c and $\zeta_{S_1}(t)$ with different initial conditions. (d) Basin of attraction region of system (2) when $y_{12} < \rho T_s$ while the all the orbits starting from the blue domains will tend to the pseudo-equilibrium E_c and any orbit initiating from the green domains will tend to virus-free periodic solution $\zeta_{S_1}(t)$. The other parameter values are fix as those in Fig. 5(a). (For interpretation of the references to color in this figure legend, the reader is referred to the web version of this article.)

Fig. 8(d)), and then we can conclude that

$$\cdots \to \overline{F_{n-1}G_n} \to \overline{F_{n-2}G_{n-1}} \to \cdots \to \overline{P_2G_1} \to \overline{P_7'P_{16}} \to \zeta_{S_1}(t),$$

and

$$\cdots \to \overline{G_nF_n} \to \overline{G_{n-1}F_{n-1}} \to \cdots \to \overline{G_1F_1} \to \overline{P_{16}P_2} \to E_c.$$

Therefore, the dynamics of system (2) when $\rho T_s > y_{12}$ can be concluded as the follows.

Theorem 9. *When $\rho T_s > y_{12}$, then the virus-free periodic solution $\zeta_{S_1}(t)$ and the pseudo-equilibrium E_c are bistable (see Fig. 9(a–c)). And both of them have a basin of attraction $D_{P_{16}^2} \cup D_{P_2G_1} \cup D_{F_nG_{n+1}}$ and $D_\Upsilon \cup D_{G_nF_n}$ $(n = 1, 2, \ldots)$ respectively (as shown in Fig. 9(d)).*

Remark 4. In the above discussions on the domains of attraction of system (2), there exist two special cases that the orbits initiating from the two intersection points of the line $y = \rho T_s$ with the curve Υ will tend to the equilibrium $E_{S_2}^2$. Therefore, all the domains of attraction should get rid of countable orbits which can approach the two intersection points. In details, for Theorem 5, we should get rid of the orbits Γ_{A_n} and the curve Υ, while the orbits Γ_{A_n}, Γ_{C_n} and the curve Υ should be deleted in Theorem 6. And for Theorems 7–9, we should get rid of the orbits Γ_{G_n}, Γ_{F_n} and the curve Υ in the domains of attraction.

Remark 5. It should be noted that we have not obtained theoretical results for $y_{11} < \rho T_s < y_{10}$ or $y_{13} < \rho T_s < y_{12}$. However, numerical studies show that the dynamics of system (2) for $y_{11} < \rho T_s < y_{10}$ are similar to the case $y_8 < \rho T_s < y_{11}$, as shown in Fig. 10(a), that is, the pseudo-equilibrium E_c is globally stable. It is difficult to theoretically prove this conclusion because we can not determine the sign of the function $\Phi(x^0) - x^0, x^0 \in (x_6, x_7)$. For $y_{13} < \rho T_s < y_{12}$, numerical studies suggest the dynamics of system (2) are similar to those for the case $\rho T_s > y_{12}$, that is, the pseudo-equilibrium E_c and the virus-free periodic solution $\zeta_{S_1}(t)$ are bistable in their basin of attraction regions as shown in Fig. 10(b–d).

5. Conclusion and discussion

In this paper, considering combined antiretroviral therapy and interleukin (IL)-2 treatment with impulsive immune therapy for HIV infected patients, we proposed a piecewise virus-immune model with two thresholds to describe the HIV-1 RNA virus and effector cell guided STI therapy. The model allows us to determine under what threshold values of the density of the effector cells and HIV-1 RNA virus loads we can successfully inhibit the growth of the virus and rebuild the immune response function of the HIV infected patients. We extended our previously formulated model [17] by including impulsive immune therapy.

The immune therapy has been shown to be effective in helping to rebuild the HIV-special immune response. We initially discussed the dynamics of system (2) when only the effector cell-guided therapy is considered (i.e. systems (5) and (6)). Our theoretical analysis shows the existence and local stability of the virus-free periodic solution when ρT_s exceeds the critical value $y_{q_{S_1}}^u$ for system (5) or $y_{q_{S_2}}^u$ for system (6). It means that the HIV-1 RNA virus can be eradicated by infinite times of impulsive immune therapy if efficacy of immune therapy is relatively high. If the virus-free periodic solution becomes unstable (i.e. $y_{S_1}^l < \rho T_s < y_{q_{S_1}}^u$

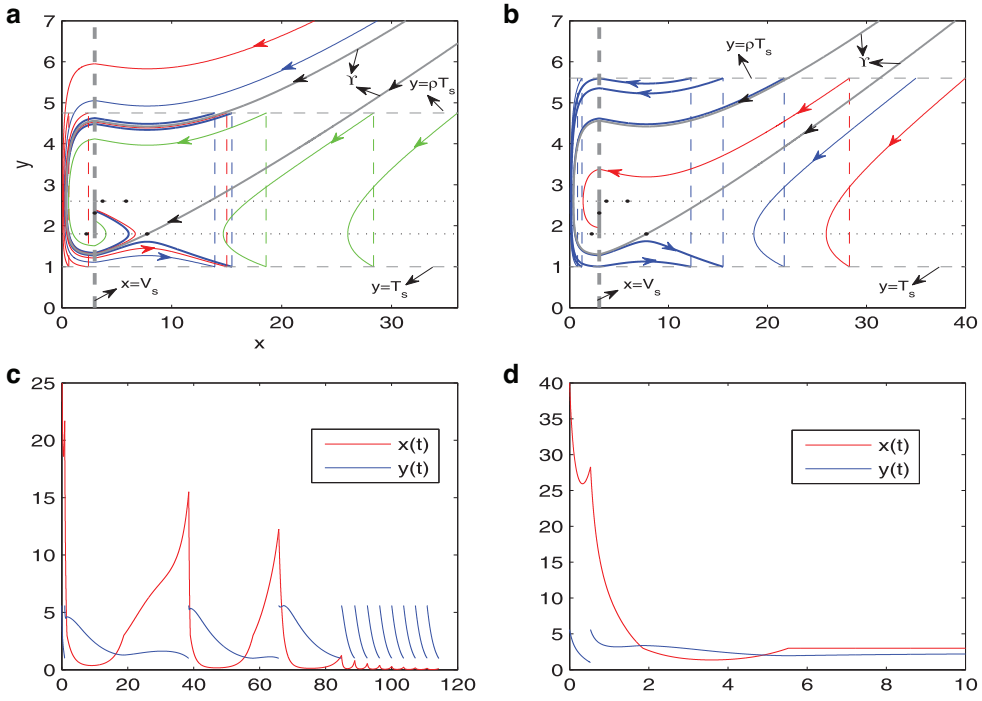

Fig. 10. (a) The dynamic behaviors of system (2) when $y_{11} < \rho T_s < y_{10}$ with $\rho = 4.75$; (b) The dynamic behaviors of system (2) when $y_{13} < \rho T_s < y_{12}$ with $\rho = 5.6$; (c) The solution trajectory of system (2) when $y_{13} < \rho T_s < y_{12}$, which tend to the virus-free periodic solution $\zeta_{S_1}(t)$; (d) The solution trajectory of system (2) when $y_{13} < \rho T_s < y_{12}$, which tend to the pseudo-equilibrium E_c. The other parameter values are fixed as those in Fig. 5(a).

or $y^l_{S_2} < \rho T_s < y^u_{q_{S_2}}$ holds true), then the viral loads may increase to infinity, depending on the initial conditions. This indicates that if the efficacy of impulsive immune therapy is relatively low, HIV virus may be controlled by the impulsive immune therapy only for some patients whose initial data for viral loads and effector cells satisfy certain conditions.

We also considered the piecewise model of virus-immune system with only HIV-1 RNA-guided therapy in p aper [17] and observed that virus may be maintained to be a relatively low level (e.g. the pseudo-equilibrium E_c can be locally stable in region D_γ) for $x^1_{S_2} < V_s < x^1_{S_1}$. This means that virus can not be eradicated by HIV-1 RNA-guided therapy only. Here we also examined the global dynamics of system (2) when the strategies of both the effector cell and HIV-1 RNA-guided therapy are considered, and when we further fix the threshold V_s between $x^1_{S_1}$ and $x^1_{S_2}$ and the threshold T_s below $\min\{y^l_{S_1}, y^l_{S_2}\}$. Complex and multiple attractors appear in the system (2) if we vary value of ρ and fixed other parameter values. The complex dynamics includes: (a) the pseudo-equilibrium E_c is locally stable in a basin of attraction while the orbits starting from the other region will tend to $\overline{[T_s, \rho T_s]^\infty}$; (b) the pseudo-equilibrium E_c is globally stable; (c) the pseudo-equilibrium E_c coexists with a positive order-1 periodic solution, and both of them are locally stable in their basins of attraction; (d) the pseudo-equilibrium E_c and the virus-free periodic solution $\zeta_{S_1}(t)$ are bistable in their corresponding domains of attraction, respectively.

In 1994, Kuznetsov et al. investigated similar basic ODE model with the carrying capacity of the virus loads being considered [14]. In that paper they considered the continuous therapy for immunogenic tumors. As discussed by the authors, the main theoretical results can also be applied for HIV therapy while two positive equilibria can be bistable. Compared with the continuous therapy, as we can see, the dynamics of the system with the comprehensive therapy strategies becomes very different and more rich. The pseudo-equilibrium can be bistable with the positive order-1 periodic solution or with the virus free periodic solution, and moreover their domains of attraction can be very complicated. This indicates that the outcomes for the patients under the therapy is very sensitive to their initial conditions.

Comparing with the strategies of both the effector cell and HIV-1 RNA-guided therapy with the HIV-1 RNA-guided therapy only [17], we obtained that the pseudo-equilibrium E_c can be globally stable under appropriate conditions. In contrast, the pseudo-equilibrium E_c can only be locally stable under the corresponding conditions when HIV-1 RNA-guided therapy alone is implemented (see paper [17]). This indicates that under such combined therapy strategies virus loads can be successfully controlled to remain at a certain level for all the HIV infected patients no matter what their initial conditions are. As we can see, the region D_γ can be regarded as the controllable region when HIV-1 RNA-guided therapy alone is considered, in which the virus can be maintained under a certain level. Theorems 5 and 6 imply that the controllable region is enlarged under the combined two thresholds therapy strategies, compared to the controllable region under the HIV-1 RNA-guided therapy only. Moreover, it is interesting to note that both the pseudo-equilibrium E_c and the virus-free periodic solution can be bistable if the efficacy of immune therapy is relatively high. It suggests that in such a scenario virus may be either successfully eradicated or maintained under a certain level with the two thresholds therapy strategies.

Similarly, a comparison of the strategies of both the effector cell and HIV-1 RNA-guided therapy with the effector cell-guided immune therapy only yields some interesting results about how to carry out the immune therapy. Under the effector cell-guided therapy alone, a lifelong time of impulsive immune therapy is needed to successfully control the virus load to under a relative low level and once the immune therapy blacking out the virus loads will grow again to infinity no matter how low the virus loads were controlled. However, if we consider both the effector cell and HIV-1 RNA-guided therapy, the pseudo-equilibrium E_c is globally stable when $y_8 < \rho T_s < y_{11}$. In such a situation, all orbits starting out

of the domain D_Y will jump into the region D_Y after finite times of impulsive effects and finally tend to E_c. Therefore, the patients just need finite times of immune therapy or do not require any immune therapy to control the virus loads below a certain level, depending on their initial conditions. But, if we further enhance the intensity of immune therapy, a result contrary to intuition occurs. That is, when $y_{10} < \rho T_s < y_{13}$, a locally stable positive periodic solution appears, which means that infinite times of immune therapy may also be needed to control the virus load between a range under the comprehensive two thresholds therapy strategies.

It is worth mentioning that the work presented here is an extension of an approach to the dynamics of HIV management when plasma HIV-1 RNA-guided therapy is initiated [17]. By further including effector cell-guided therapy, our analyses indicate that HIV viral loads can either be eradicated or stabilize at a previously given level or go to infinity (corresponding to the effector cells oscillating), depending on the threshold levels and the initial HIV virus loads and effector cell counts. Therefore, our findings suggest that it is essential to carefully choose the thresholds of plasma HIV-1 RNA copies and effector cell and individualize the STIs for patients based on their initial plasma HIV-1 RNA copies and effector cell counts.

In previous studies of modeling disease therapy, the Filippov system and impulsive system are usually two independent frameworks [16,24,25,29,33]. In this paper, we proposed a mathematical model combining the Filippov system and the state dependent impulsive system with two different strategies for HIV therapy considered. Our discussion of the global dynamics of system (2) shows that the dynamics becomes very rich and complicated when two different therapy strategy is considered. Our approach can not only be applied to the HIV therapy, but also modeling other disease therapies, such as cancer therapies.

When discussing the global dynamics of system (2), we can not theoretically determine the sign of the function $\Phi(x^0) - x^0$. The complexity of this function leads to difficulties to completely examine the dynamics of system (2) for cases $y_{11} < \rho T_s < y_{10}$ and $y_{13} < \rho T_s < y_{12}$. To investigate the global dynamics of system (2), we have fixed the two thresholds as $T_s < \min\{y^l_{S_1}, y^l_{S_2}\}$ and $x^1_{S_2} < V_s < x^1_{S_1}$. The dynamics of system (2) could be very complex if we choose different combinations of the two thresholds T_s and V_s. The discussion of those complex dynamics is left for us in the future works. In this paper, we have assumed that the HIV virus increases exponentially. When there is a limitation of the virus growth, it is reasonable to taking into consideration of the carrying capacity of the HIV virus. This consideration would have great influence on the dynamics of systems S_1 and S_2 and further on the dynamics of the virus-immune system with complex therapy strategies. Addressing this complexity would require a further in-depth research.

Acknowledgments

The work was supported by the national Megaproject of Science Research (No. 2012ZX10001-001), by the National Natural Science Foundation of China (NSFC, 11571273), by the Fundamental Research Funds for the Central Universities (08143042 (YX)), and by the International Development Research Center, Ottawa, Canada (104519–010).

Appendix

Lemma 2. *For $i = 1, 2$, let $x^1_{S_i} \le x_k \le x^2_{S_i}$, Γ_{k_1} and Γ_{k_2} being two orbits of system S_i outside the domain bounded by $\Gamma^1_{S_i}$, $\Gamma^2_{S_i}$ and $\Gamma^3_{S_i}$. Denote the intersection point of the line $x = x_k$ with the upper branch and the low branch of the orbit Γ_{k_1} as $P^u_{k_1}(x_k, y^u_{k_1})$ and $P^l_{k_1}(x_k, y^l_{k_1})$. Similar denote the two intersection points between the line $x = x_k$ and the orbit Γ_{k_2} as $P^u_{k_2}(x_k, y^u_{k_2})$ and $P^l_{k_2}(x_k, y^l_{k_2})$. Then there should be three intersection points of the line $y = y^u_{k_1}$ to the orbit Γ_{k_1} and we denote the one with the biggest horizontal ordinate as $P'^u_{k_1} = (x'^u_{k_1}, y^u_{k_1})$. Similarly, we can denote the three other points $P'^l_{k_1} = (x'^l_{k_1}, y^l_{k_1})$, $P'^u_{k_2} = (x'^u_{k_2}, y^u_{k_2})$ and $P'^l_{k_2} = (x'^l_{k_2}, y^l_{k_2})$. Then we have $x'^u_{k_1} = x'^u_{k_2} = x'^l_{k_1} = x'^l_{k_2}$.*

Proof. Without loss of generality, we just verify $x'^u_{k_1} = x'^u_{k_2}$ for system S_1. As shown in the proof of Lemma 1, there is

$$\left(\frac{c}{1+\omega x} - q - \frac{\delta}{x}\right)dx = \left(\frac{r}{y} - p\right)dy. \tag{19}$$

Integrating Eq. (19) from $E^u_{k_1}$ to $E'^u_{k_1}$ yields:

$$\int_{x_k}^{x'^u_{k_1}} \left(\frac{c}{1+\omega x} - q - \frac{\delta}{x}\right)dx = \int_{y^u_{k_1}}^{y^u_{k_1}} \left(\frac{r}{y} - p\right)dy = 0, \tag{20}$$

and from $E^u_{k_2}$ to $E'^u_{k_2}$ we have

$$\int_{x_k}^{x'^u_{k_2}} \left(\frac{c}{1+\omega x} - q - \frac{\delta}{x}\right)dx = \int_{y^u_{k_2}}^{y^u_{k_2}} \left(\frac{r}{y} - p\right)dy = 0. \tag{21}$$

Combining Eqs. (20) and (21) there is

$$\int_{x_k}^{x'^u_{k_1}} \left(\frac{c}{1+\omega x} - q - \frac{\delta}{x}\right)dx = \int_{x_k}^{x'^u_{k_2}} \left(\frac{c}{1+\omega x} - q - \frac{\delta}{x}\right)dx, \tag{22}$$

which implies that $x'^u_{k_1} = x'^u_{k_2}$. The proof is completed. □

Lemma 3. *Let $M(x_M, y_M)$ being a point in $\{(x, y)|x > 0, y > 0\}$ with $y_M < y^1_{S_2}$, $\Gamma^M_{S_1}$ and $\Gamma^M_{S_2}$ being the orbits of systems S_1 and S_2 passing through the point M, respectively. Denote the another intersection points of the orbits $\Gamma^M_{S_1}$ and $\Gamma^M_{S_2}$ to the line $x = x_M$ as $M_{S_1}(x_M, y_{M_{S_1}})$ and $M_{S_2}(x_M, y_{M_{S_2}})$ respectively. Then we have that $y_{M_{S_1}} < y_{M_{S_2}}$.*

Proof. Similar to system S_1, the system S_2 has the first integral which is given as

$$\begin{aligned} H_2(x, y) = &-\frac{c}{\omega}\ln(1+\omega x) + (\delta - \epsilon_2)\ln(x) \\ &+ qx + (r - \epsilon_1)\ln(y) - py = h_2, \end{aligned} \tag{23}$$

where $h_2 = H_2(x_2, y_2)$ is a constant. Also, there are

$$\begin{aligned} y^{S_2}_l = &-\frac{r-\epsilon_1}{p} W\Bigg[0, -\frac{p}{r-\epsilon_1}\exp \\ &\times\left(\frac{c\ln(1+\omega x) - (\delta-\epsilon_2)\omega\ln(x) - q\omega x + h_2\omega)}{(r-\epsilon_1)\omega}\right)\Bigg] \end{aligned} \tag{24}$$

and

$$\begin{aligned} y^{S_2}_u = &-\frac{r-\epsilon_1}{p} W\Bigg[-1, -\frac{p}{r-\epsilon_1}\exp \\ &\times\left(\frac{c\ln(1+\omega x) - (\delta-\epsilon_2)\omega\ln(x) - q\omega x + h_2\omega)}{(r-\epsilon_1)\omega}\right)\Bigg]. \end{aligned} \tag{25}$$

According the Eqs. (14) and (25), we have that

$$\begin{aligned} y_{M_{S_1}} = &-\frac{r}{p} W\Bigg[-1, -\frac{p}{r}\exp \\ &\times\left(\frac{c\ln(1+\omega X_M) - \delta\omega\ln(X_M) - q\omega X_M + h_{M_{S_1}}\omega)}{r\omega}\right)\Bigg] \end{aligned} \tag{26}$$

and

$$y_{M_{S_2}} = -\frac{r-\epsilon_1}{p} W\left[-1, -\frac{p}{r-\epsilon_1}\exp \times\left(\frac{c\ln(1+\omega X_M)-(\delta-\epsilon_2)\omega\ln(X_M)-q\omega X_M+h_{M_{S_2}}\omega)}{(r-\epsilon_1)\omega}\right)\right]. \tag{27}$$

where $h_{M_{S_1}} = H_1(x_M, y_M)$ and $h_{M_{S_2}} = H_2(x_M, y_M)$. Simplifying Eqs. (26) and (27) yields:

$$y_{M_{S_1}} = -\frac{r}{p} W\left[-1, -\frac{p}{r}\exp\left(\ln(y_M)-\frac{p}{r}y_M\right)\right] \tag{28}$$

and

$$y_{M_{S_2}} = -\frac{r-\epsilon_1}{p} W\left[-1, -\frac{p}{r-\epsilon_1}\exp\left(\ln(y_M)-\frac{p}{r-\epsilon_1}y_M\right)\right]. \tag{29}$$

Let

$$f(\epsilon_1) = \frac{\frac{p}{r}\exp\left(\ln(y_M)-\frac{p}{r}y_M\right)}{\frac{p}{r-\epsilon_1}\exp\left(\ln(y_M)-\frac{p}{r-\epsilon_1}y_M\right)} = \frac{r-\epsilon_1}{r}\exp \times\left(y_M\left(\frac{p}{r-\epsilon_1}-\frac{p}{r}\right)\right). \tag{30}$$

It follows from $y_M < y^1_{S_2} = \frac{r-\epsilon_1}{p}$ that

$$f(\epsilon_1) < \frac{r-\epsilon_1}{r}\exp\left(\frac{r-\epsilon_1}{p}\left(\frac{p}{r-\epsilon_1}-\frac{p}{r}\right)\right) = \frac{r-\epsilon_1}{r}\exp\left(\frac{\epsilon_1}{r}\right) = g(\epsilon_1). \tag{31}$$

Definitely, there is $g'(\epsilon_1) < 0$, which implies that $g(\epsilon_1) < g(0) = 1$.

That means

$$-\frac{p}{r}\exp\left(\ln(y_M)-\frac{p}{r}y_M\right) > -\frac{p}{r-\epsilon_1}\exp\left(\ln(y_M)-\frac{p}{r-\epsilon_1}y_M\right). \tag{32}$$

Then according to the properties of the Lambert W function we have

$$W\left[-1, -\frac{p}{r}\exp\left(\ln(y_M)-\frac{p}{r}y_M\right)\right] < W\left[-1, -\frac{p}{r-\epsilon_1}\exp \times\left(\ln(y_M)-\frac{p}{r-\epsilon_1}y_M\right)\right]. \tag{33}$$

which means that there is $y_{M_{S_1}} > y_{M_{S_2}}$. This completes the proof. □

References

[1] A. Carr, K. Samaras, A. Thorisdottir, G.R. Kaufmann, D.J. Chisholm, D.A. Cooper, Diagnosis, prediction, and natural course of HIV-1 protease-inhibitor-associated lipodystrophy, hyperlipidaemia, and diabetes mellitus: a cohort study, Lancet 353 (1999) 2093–2099.

[2] M. Harrington, C. Carpenter, Hit HIV-1 hard, but only when necessary, Lancet 355 (2000) 2147–2152.

[3] V.A. Johnson, F. Brun-Vezinet, B. Clotet, B. Conway, et al., Update of the drug resistance mutations in HIV-1: 2004, Topics HIV Med. 12 (2004) 119–124.

[4] L. Zhang, B. Ramratnam, K. Tenner-Racz, et al., Quantifying residual HIV-1 replication in patients receiving combination antiretroviral therapy, New Engl. J. Med. 340 (1999) 1605–1613.

[5] F. Maggiolo, M. Airoldia, A. Callegaro, et al., CD4 cell-guided scheduled treatment interruptions in HIV-infected patients with sustained immunologic response to HAART, AIDS 23 (2009) 799–807.

[6] J. Anaworanich, R. Nuesch, M.L. Braz, et al., CD4 guided scheduled treatment interruption compared to continuous therapy: results of the staccato trial, Lancet 368 (2006) 459–465.

[7] W.M. EL-Sadr, J.D. Lundgren, J.D. Neaton, et al., CD 4^+ count-guided interruption of antiretroviral treatment. the strategies for management of antiretroviral therapy study group, New Engl. J. Med. 355 (2006) 2283–2296.

[8] M.L.G. Fernandez, P. Rivas, M. Molina, R. Garcia, M. De Gorgolas, Long-term follow-up of asymptomatic HIV-infected patients who discontinued antiretroviral therapy, Clin. Infect. Dis. 41 (2005) 390–394.

[9] M.M. Hadjiandreou, R. Conejeros, D.I. Wilson, Long-term HIV dynamics subject to continous therapy and structured treatment interruption, Chem. Eng. Sci. 64 (2009) 1600–1617.

[10] F. Lori, R. Maserati, A. Foli, et al., Structured treatment interruptions to control HIV-1 infection, Lancet 355 (2000) 287–288.

[11] F. Maggiolo, D. Ripamonti, A. Grellegaro, et al., Effect of prolonged discontinuation of successful antiretroviral therapy on CD4 cells, a controlled, prospective trial, AIDS 18 (2004) 439–446.

[12] L. Ruiz, R. Paredes, G. Gómez, J. Romeu, et al., Antiretroviral therapy interruption guided by CD4 cell counts and plasma HIV-1 RNA levels in chronically HIV-1-infected patients, AIDS 21 (2007) 169–178.

[13] S.M. Blower, H.B. Gershengorn, R.M. Grant, Grant a tale of two futures: HIV and antiretroviral therapy in san francisco, Science 287 (2007) 650–654.

[14] V.A. Kuznetsov, I.A. Makalkin, M.A. Taylor, A.S. Petelson, Nonlinear dynamics of immunogenic tumors: parameter estimation and global bifurcation analysis, Bull. Math. Biol. 56 (2) (1994) 295–321.

[15] Y.N. Xiao, H.Y. Miao, S.Y. Tang, H.L. Wu, Modeling antiretroviral drug responses for HIV-1 infected patients using differential equation models, Adv. Drug Deliver. Rev. 65 (2013) 940–953.

[16] S.Y. Tang, Y.N. Xiao, N. Wang, H.L. Wu, Piecewise HIV virus dynamic model with CD 4^+ t cell count-guided therapy: I, J. Theor. Biol. 308 (2012) 123–134.

[17] B. Tang, Y.N. Xiao, R.A. Check, N. Wang, A piecewise model of virus-immune dynamics with HIV-1 RNA guided therapy, J. Theor. Biol. 377 (2015) 36–46.

[18] G.A.D. Hardy, N. Imami, M.R. Nelson, et al., A phase i, randomized study of combined IL-2 and therapeutic immunisation with antiretroviral therapy, J. Immune. Based Ther. Vaccines 5 (2007) 6.

[19] M.D. Bernardo, C.J. Budd, A.R. Champneys, P. Kowalczyk, A.B. Nordmark, G.O. Tost, P.T. Pllrolnen, Bifurcations in nonsmooth dynamical system, SIAM Review 50 (4) (2008) 629–701.

[20] A.K. Yu, S. Rinaldi, A. Grafnani, One parameter bifurcations in planar filippov systems, Inter. J. Bif. Chaos 13 (2003) 2157–2188.

[21] C. Padmanabhan, R. Singh, Dynamics of a piecewise nonlinear system subject to dual harmonic excitation using parametric continuation, J. Sound. Vib. 184 (5) (1995) 767–799.

[22] S.Y. Tang, J.H. Liang, Y.N. Xiao, R.A. Check, Sliding bifurcations of filippov tow stage pest control models economic thresholds, SIAM J. Appl. Math. 72 (4) (2012) 1061–1080.

[23] S.Y. Tang, J.H. Liang, Global qualitative analysis of a non-smooth gause predator-prey model with a refuge, Nonlinear Anal. TMA 76 (2013) 165–180.

[24] Y.N. Xiao, T.T. Zhao, S.Y. Tang, Dynamics of an infectious disease with media/psychology induced non-smooth incidence, Math. Biosci. Eng. 10 (2013) 445–461.

[25] Y.N. Xiao, X.X. Xu, S.Y. Tang, Sliding mode control of outbreaks of emerging infectious diseases, Bull. Math. Biol. 74 (2012) 2403–2422.

[26] Y.N. Xiao, S.Y. Tang, J.H. Wu, Media impact switching surface during an infectious disease outbreak, Sci. Rep. 5 (2015), doi:10.1038/srep07838.

[27] E.M. Bonotto, M. Federson, Limit sets and the poincaré bendixson theorem in impulsive semidynamical systems, J. Differ. Equ. 244 (2008) 2334–2349.

[28] E.M. Bonotto, Lasalle's theorems in impulsive semidynamical system, Nonlinear Anal. TMA 71 (2009) 2291–2297.

[29] L.F. Nie, Z.D. Teng, B.Z. Guo, A state dependent pulse control strategy for a SIRS epidemic system, Bull. Math. Biol. 75 (2013) 1697–1715.

[30] S.Y. Tang, R.A. Cheke, State-dependent impulsive models of integrated pest management (IPM) strategies and their dynamic consequences, J. Math. Biol. 50 (2005) 227–240.

[31] S.Y. Tang, B. Tang, A.L. Wang, Y.N. Xiao, Holling II predator-prey impulsive semi-dynamic model with complex poincaré map, Nonlinear Dyn. 81 (2015) 1575–1596.

[32] G.Z. Zeng, L.S. Chen, I.H. Sun, Existence of periodic solution of order of one planar impulsive autonomous system, J. Comp. Appl. Math. 186 (2006) 466–481.

[33] S.Y. Tang, W.H. Pang, R.A. Check, J.H. Wu, Global dynamics of a state-dependent feedback control system, Adv. Differ. Equ. 2015 (2015) 322.

[34] R.M. Corless, G.H. Connet, D.E.G. Hare, D.J. Jeffrey, D.E. Knuth, On the lambert w function, Adv. Comput. Math. 5 (1996) 329–359.